

RECEIVED: September 9, 2024

ACCEPTED: December 9, 2024

PUBLISHED: January 21, 2025

Measurement of inclusive and differential cross sections of single top quark production in association with a W boson in proton-proton collisions at $\sqrt{s} = 13.6 \text{ TeV}$



The CMS collaboration

E-mail: cms-publication-committee-chair@cern.ch

ABSTRACT: The first measurement of the inclusive and normalised differential cross sections of single top quark production in association with a W boson in proton-proton collisions at a centre-of-mass energy of 13.6 TeV is presented. The data were recorded with the CMS detector at the LHC in 2022, and correspond to an integrated luminosity of 34.7 fb^{-1} . The analysed events contain one muon and one electron in the final state. For the inclusive measurement, multivariate discriminants exploiting the kinematic properties of the events are used to separate the signal from the dominant top quark-antiquark production background. A cross section of $82.3 \pm 2.1(\text{stat})^{+9.9}_{-9.7}(\text{syst}) \pm 3.3(\text{lumi}) \text{ pb}$ is obtained, consistent with the predictions of the standard model. A fiducial region is defined according to the detector acceptance to perform the differential measurements. The resulting differential distributions are unfolded to particle level and show good agreement with the predictions at next-to-leading order in perturbative quantum chromodynamics.

KEYWORDS: Hadron-Hadron Scattering, Top Physics

ARXIV EPRINT: [2409.06444](https://arxiv.org/abs/2409.06444)

Contents

1	Introduction	1
2	The CMS detector and event reconstruction	3
3	Data and simulated samples	5
4	Event selection	7
5	Methodology for the inclusive measurement	8
6	Methodology for the differential measurements	12
7	Systematic uncertainties	15
7.1	Experimental uncertainties	17
7.2	Modelling uncertainties	18
7.3	Background normalisation uncertainties	20
8	Results	20
8.1	Inclusive measurement	20
8.2	Normalised fiducial differential cross section measurements	22
9	Summary	25
The CMS collaboration		34

1 Introduction

The three main production modes of single top quarks in proton-proton (pp) collisions are mediated via electroweak interactions and are commonly categorised through the virtuality of the exchanged W boson. When the four-momentum of the W boson is space-like, the process is referred to as the t channel, while when it is time-like, the process is referred to as the s channel. The third production mode, referred to as the tW process, is characterised by the production of a top quark in association with an on-shell W boson. The study of this production mechanism is interesting due to its interference with top quark pair ($t\bar{t}$) production [1–3], its sensitivity to standard model (SM) parameters, such as the V_{tb} Cabibbo-Kobayashi-Maskawa matrix element and the contribution of the bottom quark to the proton parton distribution functions (PDFs) [4, 5]. It is also sensitive to physics beyond the SM [6–12] and plays an important role as a background in several other analyses. One example is the recent inclusive $t\bar{t}$ cross section measurement at $\sqrt{s} = 13.6$ TeV from the CMS Collaboration [13] or at 13 TeV from the ATLAS Collaboration [14], where the uncertainty in the tW cross section is one of the leading uncertainties. The tW production rate is sufficiently high to perform a measurement of the production cross section differentially as a function

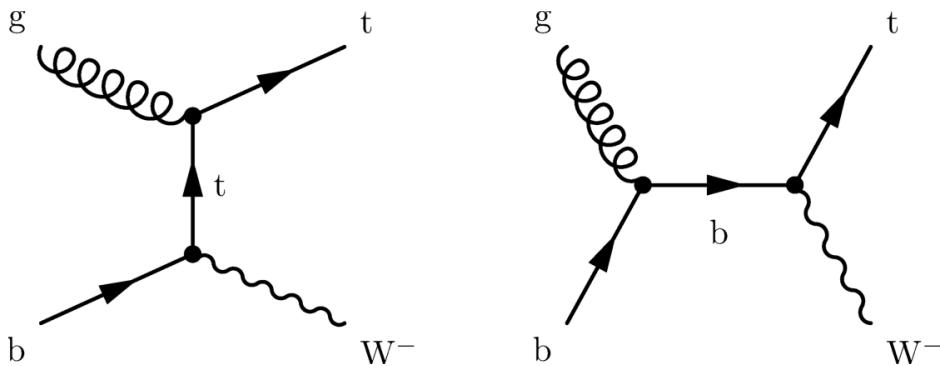


Figure 1. Leading-order Feynman diagrams of single top quark production in the tW mode. The charge-conjugate modes are implicitly included.

of various kinematic observables. These measurements are crucial to study the modelling of the tW process in perturbative quantum chromodynamics (QCD).

The associated production of a top quark and a W boson involves the electroweak interaction of a bottom quark with a W boson. At leading order (LO) in perturbative QCD (pQCD) the final state contains a W boson and, after the decay of the top quark, an additional W boson and a bottom quark. The LO Feynman diagrams for tW production are shown in figure 1. At next-to-LO (NLO) in pQCD, the tW process can contain an additional bottom quark and interferes with $t\bar{t}$ production [1–3]. The predicted cross section of tW production in pp collisions at $\sqrt{s} = 13.6$ TeV is $\sigma_{tW}^{\text{SM}} = 87.9^{+2.0}_{-1.9}$ (scale) ± 2.4 (PDF+ α_S) pb (where α_S is the strong coupling constant) and was computed at approximate next-to-next-to-NLO accuracy ($aN^3\text{LO}$) in pQCD with the addition of next-to-next-to-next-to-leading logarithmic resummation of soft-gluon emission terms [15–17]. A top quark mass (m_t) of 172.5 GeV and the PDF4LHC21 PDF set [18] were used. The quoted uncertainties include the uncertainty from varying the renormalisation (μ_R) and factorisation (μ_F) scales, the choice of PDFs, and the α_S value used by the PDF set, respectively.

The first observation of electroweak production of single top quarks was achieved by the D0 [19] and CDF [20] Collaborations at the Fermilab Tevatron. Their observations are consistent with the SM expectations for the t and s channels. The tW channel was not observed at the Tevatron due to its small cross section in proton-antiproton collisions at $\sqrt{s} = 1.96$ TeV. At the LHC, however, it represents the second-largest single top quark production mode after the t channel. The ATLAS and CMS Collaborations presented the first evidence for the tW production at 7 TeV [21, 22] and its observation at 8 TeV [4, 23]. The inclusive tW production cross section has also been measured by the ATLAS and CMS experiments at 13 TeV using data recorded during 2016 [24, 25] and using data recorded during 2015–2018 [26, 27]. Measuring the inclusive and differential tW production cross sections presents particular challenges due to the dominant background from $t\bar{t}$ events, constituting approximately 80% [28] of the total number of events in the most tW -enriched category with two leptons and one jet identified as coming from the fragmentation of a bottom quark. The first measurement of the differential cross section of tW production was carried out by the ATLAS experiment [28]. Additionally, a study [29] investigating the $WWbb$ signature (that

includes tW and $t\bar{t}$) was done by the ATLAS Collaboration. The CMS experiment has also published differential cross section measurements [27] at $\sqrt{s} = 13$ TeV using data recorded during the 2016–2018 period. Recent studies in the lepton+jets channel have been conducted at 13 TeV by the CMS Collaboration [30] and at 8 TeV by the ATLAS Collaboration [31]. For each of these measurements, good agreement with theoretical predictions is observed.

This paper reports the first measurement of the inclusive and normalised differential tW production cross sections at $\sqrt{s} = 13.6$ TeV in dilepton final states ($e^\pm \mu^\mp$), using data collected with the CMS detector in 2022, corresponding to an integrated luminosity of 34.7 fb^{-1} . For the inclusive measurement, multivariate techniques are used to build a discriminant to separate the signal from the dominant $t\bar{t}$ background, and a maximum likelihood fit to several event categories is performed. For the differential measurements, a fiducial region is defined according to the detector acceptance. The resulting distributions are unfolded to particle level and normalised to the fiducial cross section.

The paper is structured as follows. Section 2 describes the CMS detector and event reconstruction. Section 3 provides a summary of the data and Monte Carlo (MC) samples used in the analysis. The object and event selection criteria are outlined in section 4. Sections 5 and 6 describe the signal extraction strategies for the inclusive and differential measurements, respectively. The systematic uncertainties are discussed in section 7. The results of both the inclusive and differential measurements are presented in section 8. Finally, a summary of both measurements is given in section 9. Tabulated results are provided in the HEPData record for this analysis [32].

2 The CMS detector and event reconstruction

The central feature of the CMS apparatus is a superconducting solenoid of 6 m internal diameter, providing a magnetic field of 3.8 T. Within the solenoid volume are a silicon pixel and strip tracker, a lead tungstate crystal electromagnetic calorimeter (ECAL), and a brass and scintillator hadron calorimeter (HCAL), each composed of a barrel and two endcap sections. Forward calorimeters extend the pseudorapidity (η) coverage provided by the barrel and endcap detectors. Muons are measured in gas-ionisation detectors embedded in the steel flux-return yoke outside the solenoid. More detailed descriptions of the CMS detector, together with a definition of the coordinate system used and the relevant kinematic variables, can be found in refs. [33, 34].

Events of interest are selected using a two-tiered trigger system. The first level, composed of custom hardware processors, uses information from the calorimeters and muon detectors to select events at a rate of around 100 kHz within a fixed latency of about $4 \mu\text{s}$ [35]. The second level, known as the high-level trigger [36], consists of a farm of processors running a version of the full event reconstruction software optimised for fast processing, and reduces the event rate to around 5 kHz before data storage [37].

During the second long shutdown initiated in 2018, the CMS experiment underwent numerous upgrades and improvements to the subdetectors, readout electronics, trigger, data acquisition, software, and offline computing systems. Notable examples include new silicon photomultipliers and readout electronics for the HCAL that allow for a finer granularity and longitudinal segmentation [38], the replacement of the innermost layer of the silicon pixel

detector [39], the new hybrid farm of central processing units and graphics processing units for the high-level trigger [40], and rebuilt dedicated online luminosity monitors [41–43].

The particle-flow (PF) algorithm [44] aims at reconstructing and identifying all stable particles in an event, with a thorough combination of all subdetector information. In this process, the identification of the particle type (photon, electron, muon, charged or neutral hadron) plays an important role in the determination of the particle direction and energy. The primary vertex (PV), which is the vertex corresponding to the hardest scattering in the event, is evaluated using tracking information alone as described in section 9.4.1 of ref. [45]. The energy of photons is obtained from the ECAL measurement. The energy of electrons is determined from a combination of the electron momentum at the interaction PV as determined by the tracker, the energy of the corresponding ECAL cluster, and the energy sum of all bremsstrahlung photons spatially compatible with originating from the electron track. To account for the observed differences between the transverse momentum (p_T) of the electron in data and simulation, the simulated p_T is corrected to match the scale and resolution of data. Muons are identified as tracks in the central tracker consistent with either a track or several hits in the muon system. The energy of charged hadrons is determined from a combination of their momentum measured in the tracker and the matching ECAL and HCAL energy deposits. Those energy deposits are corrected for the response function of the calorimeters to hadronic showers. Finally, neutral hadrons are identified as HCAL energy clusters not linked to any charged-hadron trajectory, or as a combined ECAL and HCAL energy excess with respect to the expected charged-hadron energy deposit.

Jets are reconstructed from the PF candidates using the anti- k_T clustering algorithm [46, 47] with a distance parameter of 0.4. The jet momentum is determined as the vector sum of all particle momenta in the jet. Additional pp interactions within the same or nearby bunch crossings, known as pileup, can contribute additional tracks and calorimetric energy depositions to the jet momentum. The pileup-per-particle identification algorithm (PUPPI) [48, 49] is used to mitigate the effect of pileup at the reconstructed-particle level, making use of local shape information, event pileup properties, and tracking information. A local shape variable is defined, which distinguishes between collinear and soft diffuse distributions of other particles surrounding the particle under consideration. The former is attributed to particles originating from the hard scattering and the latter to particles originating from pileup interactions. Charged particles identified as originating from pileup vertices are discarded. For each neutral particle, a local shape variable is computed using the surrounding charged particles compatible with the PV within the tracker acceptance ($|\eta| < 2.5$), and using all particles in the region outside the tracker coverage. The momenta of the neutral particles are then rescaled according to their probability to originate from the PV deduced from the local shape variable, eliminating the need for jet-based pileup corrections [49]. Corrections to the jet energy scale (JES) are derived from simulation to bring the measured response of jets to that of particle-level jets on average. In situ measurements of the momentum balance in dijet, photon+jet, Z+jet, and multijet events from data collected in 2022 are used to account for any residual differences in the JES between data and simulation. Additionally, the jet energy resolution (JER) in the simulation is corrected to reproduce that obtained from data [50–52].

The missing transverse momentum vector \vec{p}_T^{miss} is defined as the negative vector sum of transverse momenta of all reconstructed PF candidates in an event. Its magnitude is referred to as p_T^{miss} . To remove the effect of pileup, the PUPPI algorithm is also used for the computation of \vec{p}_T^{miss} [48, 49].

3 Data and simulated samples

Data from pp collisions at $\sqrt{s} = 13.6$ TeV collected in 2022 and corresponding to an integrated luminosity of 34.7 fb^{-1} are analysed. The last part of the 2022 data-taking period, approximately 27 fb^{-1} , was affected by a water leak in one wheel of the ECAL endcap. As a result, a small fraction of the wheel was turned off and did not record data. This aspect is taken into account in the object selection of the analysis and in the simulated samples, which are split into two periods. The data from the two periods are analysed separately, and appropriate per-period calibrations are applied before the data are combined for the cross section measurements.

Monte Carlo simulations are used to estimate the contributions from both signal and background processes. The tW signal samples are generated with POWHEG BOX v2 [53–55] at NLO accuracy in pQCD. The POWHEG h_{damp} parameter is set to 250 GeV [56], and the μ_R and μ_F scales are set to the top quark mass of 172.5 GeV. The five flavour scheme of the proton PDFs, where massless b quarks are considered as part of the protons, is used in the simulation of the tW and t̄t samples. In order to avoid double counting of Feynman diagrams arising from the common final states with t̄t, two schemes are introduced to define the tW signal. “Diagram removal” (DR) [2], where all NLO diagrams that are doubly resonant (i.e. that can have two top quarks on-shell) such as those in figure 2, are excluded from the signal definition; and “diagram subtraction” (DS) [2, 57], in which the cross section is modified with a gauge-invariant subtraction term, which locally cancels the contribution of t̄t diagrams. The DR scheme is used as the nominal model in this analysis. Nonetheless, the difference in the results obtained for the two schemes is also evaluated and used to assign a systematic uncertainty in the MC modelling. Both DR and DS schemes are used for comparison with the differential particle-level result. Additionally, signal samples generated with MADGRAPH5_aMC@NLO v2.9.13 [58] using the DR and DS scheme are also studied. Two additional derivations from these approaches are considered: the so-called “DR2” approach, that includes the terms corresponding to the interference between tW and t̄t processes, and an alternative way of implementing DS (later referred to as “DS dyn.”), where a dynamic factor is used to model the top quark resonance, providing a better treatment than DS in the subtraction of the off-shell t̄t contributions [59]. The HVQ generator [60] from POWHEG BOX is used to simulate t̄t at NLO in pQCD in the narrow width approximation. The POWHEG h_{damp} parameter is set to 250 GeV, and the μ_R and μ_F scales are set to $\mu_R = \mu_F = \sqrt{m_t^2 + p_{T,t}^2}$, where $p_{T,t}$ is the p_T of the top quark in the t̄t rest frame.

The NLO pQCD setup in POWHEG BOX is also used to simulate the WW, WZ, and ZZ (denoted as VV) diboson processes. The Z/ γ^* , referred to as Drell-Yan (DY), and W background samples are simulated at NLO in pQCD, with up to two jets considered in the matrix-element (ME) computation, using MADGRAPH5_aMC@NLO. Other contributions from vector boson (W, Z, and γ) production in association with t̄t events (denoted as t̄tV)

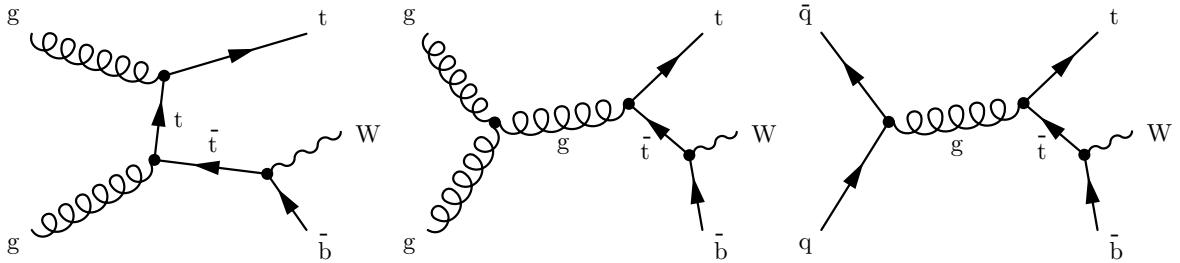


Figure 2. Representative Feynman diagrams for tW single top quark production at NLO that are removed from the signal definition in the DR scheme. The charge-conjugate modes are implicitly included.

are simulated at NLO in pQCD using `MADGRAPH5_AMC@NLO`. Finally, simulated W and $t\bar{t}$ samples with one lepton and jets in the final state are used to estimate the background contribution from events with a jet incorrectly reconstructed as a lepton (electron or muon). The latter background contributions are labelled as non- W/Z since they contain a lepton candidate that does not originate from a leptonic decay of a weak boson.

For all simulated samples, the proton structure in the ME calculation is described with the NNPDF 3.1 PDF set [61] at next-to-NLO order (NNLO). The generators are interfaced in all cases with `PYTHIA` v8.306 [62], which is used to model the hadronisation and parton showering (PS). The underlying event is modelled with the CP5 tune [63] in all samples. For comparison at the particle level, another signal sample is considered where the `POWHEG BOX` generator is interfaced with `HERWIG` v7.2.2 [64–66] using the CH3 [67] tune. For the samples generated with `MADGRAPH5_AMC@NLO`, the double counting of partons from the ME calculations and PS described by `PYTHIA` is removed using the FxFx [68] matching scheme. This is the case for the DY, W , and $t\bar{t}V$ samples. The nominal m_t is set to 172.5 GeV for all samples. For the tW signal and $t\bar{t}$ background, alternative samples were generated to estimate systematic uncertainties, which are obtained from the same generator (`POWHEG BOX`) and PS simulation (`PYTHIA`). These uncertainties are described in detail in section 7.

The `GEANT4` package [69] is used to simulate the CMS detector for all simulation samples. To compare with the measured data, the event yields in the simulated samples are normalised to the product of the integrated luminosity and the corresponding theoretical cross section. These are taken from aN³LO calculations for tW events [15–17], NNLO calculations for W production and DY [70], and NLO calculations for diboson production [71]. For the normalisation of the simulated $t\bar{t}$ samples, the full NNLO plus next-to-next-to-leading-logarithmic accuracy calculation [72], performed with the `TOP++` 2.0 program [73] with the PDF4LHC21 PDF set, is used. The PDF uncertainty is added in quadrature to the uncertainty associated with α_S to obtain a $t\bar{t}$ production cross section of $923.6^{+22.6}_{-33.4}$ (scale) ± 22.8 (PDF+ α_S) pb assuming $m_t = 172.5$ GeV.

To model the effect of pileup, additional simulated pp interactions in the same or neighbouring bunch crossings are generated with `PYTHIA` and overlapped with the simulated hard-scatter events. A reweighting is applied in simulations to match the pileup distribution observed in data. The average number of pileup interactions per bunch crossing in 2022 is 46 (assuming a total inelastic pp cross section of 80 mb).

4 Event selection

The analysis strategy exploits the fact that in the SM the top quark decays almost always into a W boson and a bottom quark. Signal tW events in which both W bosons decay leptonically are used. The events with same-flavour leptons are rejected due to high background contamination from DY events in this channel. This leads to a final state composed of two different-flavour leptons with opposite electric charge, $e^\pm \mu^\mp$, one jet resulting from the fragmentation of a bottom quark, and two neutrinos.

Events are recorded using a set of dilepton and single-lepton triggers, with lepton isolation requirements, that are looser than those applied later in the offline analysis, imposed on all of them [36]. The dilepton triggers require events to contain either one electron with $p_T > 12$ GeV and one muon with $p_T > 23$ GeV, or one muon with $p_T > 8$ GeV and one electron with $p_T > 23$ GeV. To increase the trigger efficiency, single-lepton triggers with one electron (muon) with $p_T > 32$ (24) GeV are also used. Lepton p_T thresholds in the offline analysis are chosen to be in the trigger efficiency plateau. The combined trigger efficiency is measured using data events that pass the selection criteria of the analysis, and which were collected with triggers based on the p_T imbalance in the event. On average, the trigger efficiency is about 98% for events passing the final analysis event selection and is corrected in simulated events to match that observed in data.

Further requirements are imposed on the reconstructed lepton and jet candidates obtained from the PF algorithm. For leptons, additional identification (ID) criteria are applied to identify prompt leptons originating from W and Z boson decays at the PV. These criteria also help to reduce background contributions from nonprompt leptons, such as leptons produced by hadron decays, or jets misidentified as leptons.

Electrons and muons in the event are required to have $p_T > 20$ GeV and $|\eta| < 2.4$ and pass the “tight” working point of the cut-based ID criteria described in ref. [74] for electrons and ref. [75] for muons. Electron candidates in the transition region between the barrel and endcap ECAL, corresponding to $1.444 < |\eta| < 1.566$, are ignored because of the suboptimal electron reconstruction in this region. Electrons collected in the period and the region affected by the water leak in ECAL endcap are also not considered. Additional criteria are imposed on the impact parameter of the leptons in order to ensure that they originate from the PV. In particular, muons are required to have a transverse impact parameter $|d_{xy}| < 0.2$ cm and a longitudinal impact parameter $|d_z| < 0.5$ cm. For electrons, the criterion depends on the η of the electron: $|d_{xy}| < 0.05$ cm and $|d_z| < 0.1$ cm for $|\eta| \leq 1.479$, and $|d_{xy}| < 0.1$ cm and $|d_z| < 0.2$ cm for $|\eta| > 1.479$. This helps to reduce background contributions from nonprompt leptons and pileup. Electrons and muons are also required to be isolated. The relative isolation variable is defined as the p_T sum of all reconstructed PF candidates (except the lepton itself) within a cone of fixed radius around the lepton direction, divided by the lepton p_T . The cone radius is defined in terms of the separation variable $\Delta R = \sqrt{(\Delta\eta)^2 + (\Delta\varphi)^2}$, where $\Delta\eta$ and $\Delta\varphi$ are the difference in η and azimuthal angle, respectively. For electrons, the ID criteria in ref. [74] include a requirement on the relative isolation calculated with $\Delta R < 0.3$. For muons, the “tight” requirement from ref. [75] on the relative isolation calculated with $\Delta R < 0.4$ is applied. In both cases, corrections for the residual contributions from pileup particles to the isolation sum are applied [74, 75]. Events with W bosons decaying into τ

leptons are considered as signal only if the τ leptons decay into electrons or muons that satisfy the selection requirements. In events with more than two leptons passing the selections, the two with the largest p_T are retained for further study.

Jets are required to have $p_T > 30 \text{ GeV}$ and $|\eta| < 2.4$, and to be separated from any selected lepton by $\Delta R > 0.4$. Jets reconstructed inside the ECAL region affected by the water leak are not considered. Another category of low- p_T jets, referred to as “loose jets”, is defined using the same criteria as standard jets but with p_T between 20 and 30 GeV. The differences in these lower- p_T jets between the tW and $t\bar{t}$ distributions can be exploited for their separation, with $t\bar{t}$ events generally expected to feature more loose jets. Jets are identified as coming from the fragmentation of bottom quarks (b jets) using the ROBUSTPARTICLETRANSFORMER algorithm [76–81], with a working point that yields an identification efficiency of about 80% and misidentification probabilities of about 1% for light quark and gluon jets and about 14% for charm quark jets. The ROBUSTPARTICLETRANSFORMER algorithm is a novel deep learning approach based on a transformer model architecture recently introduced for heavy-flavour tagging. The term “robust” refers to its adversarial training, which improves the behaviour of the model making it more resilient against systematic effects that were not present in the training data. It performs better than previous models such as DEEPJET [82], as described in ref. [78].

The selected events belong to the $e^\pm\mu^\mp$ final state if the two leptons with highest p_T passing the above selection criteria are an electron and a muon of opposite electric charge. The highest p_T (leading) lepton is required to have $p_T > 25 \text{ GeV}$. In addition, to reduce the contamination from low-mass resonances and DY production of τ lepton pairs with low dilepton invariant mass, the minimum invariant mass of all pairs of identified leptons (including leptons beyond the leading two) is required to be greater than 20 GeV. The remaining events are classified by the number of jets and the number of identified b jets in the event, as shown in figure 3 (left). In the following, the notation $njmb$ represents events with exactly n jets where m of them are identified as b jets. The 1j1b region corresponds to the most signal-enriched region with a signal-to-background ratio of about 16% compared to 8% in the 2j1b region. For the inclusive measurement, the information from three regions with one or two jets and one or two b jets (1j1b, 2j1b, and 2j2b) is considered, whereas for the differential measurements, only the 1j1b region is used. Figure 3 (right) shows the distribution of the number of loose jets in the 1j1b region. In order to decrease the relative contribution from the $t\bar{t}$ background, the events in the 1j1b region with zero loose jets are used for the differential measurements. The signal-to-background ratio in this region is about 20%.

5 Methodology for the inclusive measurement

A maximum likelihood fit is performed to extract the tW signal using the most signal-enriched 1j1b region together with the 2j1b category, which also contains a significant tW contribution, and the 2j2b region. This latter region contains almost purely $t\bar{t}$ events and is used in the fit to constrain its contribution. The remaining regions, which have a lower signal-to-background ratio and substantial contributions from other backgrounds, such as DY and VV + $t\bar{t}V$, do not significantly improve the precision of the analysis and are therefore not included in the fit.

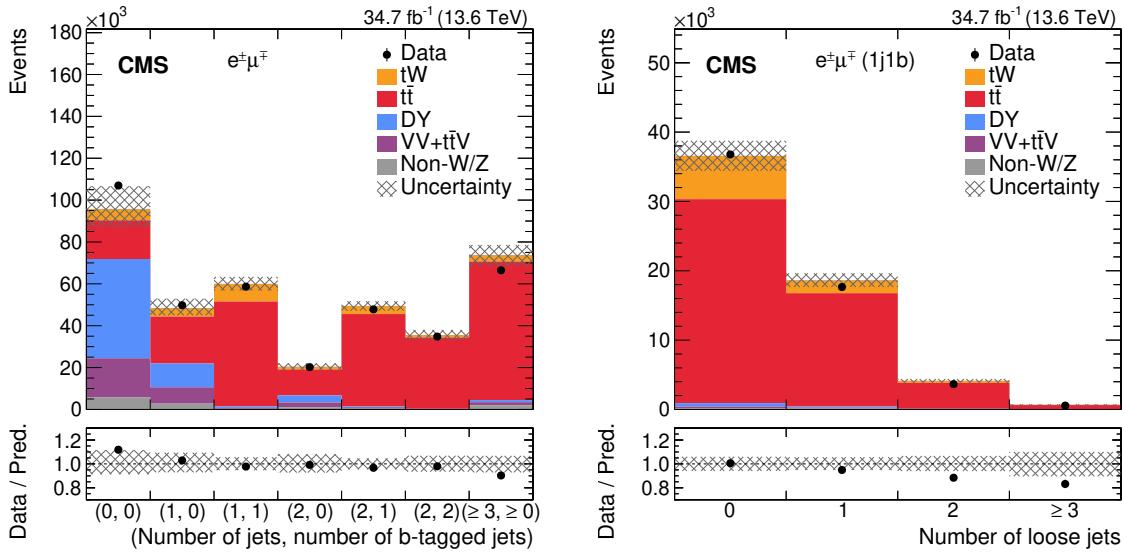


Figure 3. Left: the number of events observed in data (points) and predicted from simulation (filled histograms) in the $e^\pm\mu^\mp$ final state as a function of the number of jets and b-tagged jets before the maximum likelihood fit. Right: the number of loose jets per event in the $e^\pm\mu^\mp$ final state from the 1j1b region before the maximum likelihood fit. The vertical bars on the points show the statistical uncertainties in the data. The hatched band represents the sum of the statistical and systematic uncertainties in the MC predictions. The lower panels show the ratio of data to the sum of the expected yields.

One of the main challenges of this measurement is to distinguish the signal contribution from the dominant background contribution of $t\bar{t}$ in the dilepton final state, as there is no single observable that gives enough discrimination power between $t\bar{t}$ and tW events. To overcome this fact, two independent random forest (RF) multiclassifiers [83] implemented with the SCIKIT-LEARN package [84], one for the 1j1b region and the other for the 2j1b region, are trained to discriminate between $t\bar{t}$ in the dilepton final state, tW , and the second largest background in each category. For the 1j1b region, the second largest background is the DY process, whereas for the 2j1b region, $t\bar{t}$ with lepton+jets final states is the one that is considered. An RF classifier is an ensemble machine learning method that combines the predictions of multiple decision trees [85] to reach a single result. It improves the overall accuracy and robustness compared with single decision tree classifiers. The “random” aspect in RF comes from two sources: first, it uses a random subset of the training data for each tree (bootstrap aggregating or “bagging”), and second, it selects a random subset of features for each tree. By doing so, it reduces overfitting and increases the model’s generalizability. The final prediction is obtained by averaging all predictions of each tree. Due to the large difference in relative contribution between DY or $t\bar{t}$ in the lepton+jets final state compared with the signal and dileptonic $t\bar{t}$, RFs were chosen over boosted decision trees, as applied in ref. [27]. Random forests were found to be more robust against this particular issue, preventing any possible overfitting while keeping almost the same discrimination power. For both RFs, there are three output nodes that give the probability of a certain event to be a tW , $t\bar{t}$, or DY/lepton+jets $t\bar{t}$ event. The RFs are trained and tested using a set of simulated samples that are statistically independent from the ones used in the signal extraction. Specifically,

50% of the simulated events are allocated for training and testing, while the remaining 50% are reserved for signal extraction. Within the training and testing portion, 70% of the data is used for training while 30% is used for testing.

The input variables used in the RFs are chosen depending on their discrimination power and on how well the MC simulation models the data. The agreement between the observed data and the simulation is estimated using a goodness-of-fit test based on the saturated model [86], a model that fits the data exactly. If the p -value [87] is under 5%, the variable is rejected. For the RF in the 1j1b region, the variables used in the training in order of importance are:

- Leading loose jet p_T : if there are no loose jets, this variable is set to 0.
- Leading lepton p_T .
- $p_T(e^\pm, \mu^\mp, j)$: the magnitude of the transverse momentum of the dilepton+jet system.
- $m(e^\pm, \mu^\mp)$: invariant mass of the dilepton system.
- $\Delta\varphi(e^\pm, \mu^\mp)$: azimuthal angle between the two leptons.
- $m(e^\pm, \mu^\mp, j)$: invariant mass of the dilepton+jet system.
- $p_T(\ell_1, j)$: transverse momentum of the leading lepton+jet system.
- Jet p_T .

The order of importance is computed using the Gini importance variable [84], which measures the decrease in impurity that each feature brings when used for splitting. It computes the weighted average of the impurity decrease across all the decision points where a feature is used. The larger this decrease, the more important the feature is considered. Figure 4 shows a comparison of the observed data and simulation for the four most discriminating variables in the RF in the 1j1b region. Most of the discriminating power of the leading loose jet p_T comes from the binary decision of whether there is a loose jet in the event or not, but it also benefits from the shape information when such a jet is present. Good agreement is observed for all of them. A similar level of agreement is seen in the remaining distributions in the 1j1b region, and for the input variables of the RF trained in the 2j1b region.

The input variables listed in order of importance in the RF for the 2j1b region are:

- $m(e^\pm, \mu^\mp)$: invariant mass of the dilepton system.
- Subleading lepton p_T .
- $\Delta R(\ell_{12}, j_{12})$: separation in η - φ space between the dilepton and dijet systems.
- $p_T(e^\pm, \mu^\mp, j)$: transverse momentum of the dilepton and jet system.
- $\Delta R(e^\pm, \mu^\mp)$: angular distance in η - φ space between the two leptons.
- $\Delta R(\ell_1, j_1)$: separation in η - φ space between the leading lepton and the leading jet.

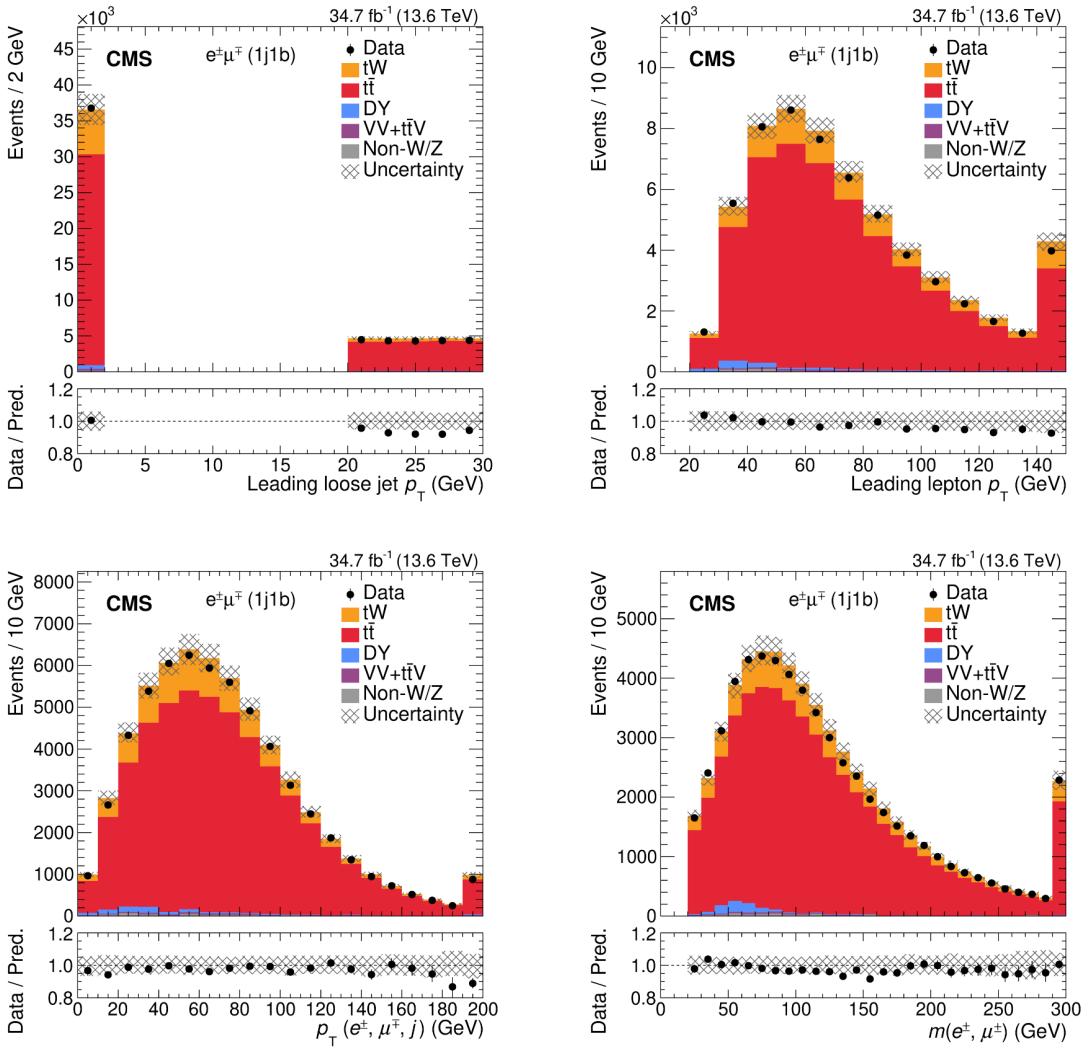


Figure 4. Distributions from data (points) and MC simulations (filled histograms) before the maximum likelihood fit of the four most discriminating variables used for the RF training of the 1j1b region: (upper left) the p_T of the leading loose jet; (upper right) the p_T of the leading lepton; (lower left) the magnitude of the transverse momentum of the dilepton+jet system; and (lower right) the invariant mass of the dilepton system. The last bin of each distribution includes the overflow events, except for the leading loose jet p_T distribution, which is only defined up to 30 GeV. The first bin in the upper left plot contains events with no loose jets. The vertical bars on the points give the statistical uncertainty in the data, and the hatched band represents the sum of the statistical and systematic uncertainties in the MC predictions. The lower panels show the ratio of the data to the sum of the MC predictions.

- $\sin \theta$: where θ is the polar angle of the total momentum of the dilepton and jet system.
- Subleading jet p_T .

The distributions that are considered in the maximum likelihood fit are the RF output distributions in the 1j1b and 2j1b regions, and the p_T distribution of the subleading jet in the 2j2b region. These distributions, before the maximum likelihood fit to the data, are shown in figure 5. All of them show good agreement between the data and prediction. The binning of the RF output distribution is chosen such that each bin contains about the same number of $t\bar{t}$ events. This avoids the presence of bins with low event counts in the background estimation, which would erroneously constrain the systematic uncertainties. The p_T distribution of the subleading jet is sensitive to JES variations and is useful in constraining this systematic uncertainty. This variable was chosen to exploit the differences between the subleading jet in tW and $t\bar{t}$. In the $t\bar{t}$ process, the subleading jet typically corresponds with the b jet from a top quark decay, while in the tW process it may be produced by additional radiation producing a less energetic jet. A simultaneous fit is performed to the three regions. The uncertainties are included using nuisance parameters, one for each source of systematic uncertainty, correlated across all regions, parameterising the effect of the given source on the expected signal and background yields.

The likelihood, $\mathcal{L}(\vec{n}|\mu, \vec{\theta})$, used in this maximum likelihood fit is a function of the observed number of events in each bin \vec{n} , the signal strength μ , defined as the ratio of the measured and expected SM cross sections $\mu = \sigma_{tW}/\sigma_{tW}^{\text{SM}}$, and a set of nuisance parameters $\vec{\theta}$ that parameterise the systematic uncertainties. It is built as the product of Poisson probabilities corresponding to the total number of events in each bin of the distributions. Furthermore, the systematic uncertainties are incorporated in the likelihood multiplied by constraint terms for each nuisance parameter θ_j given by $p_j(\theta_j)$. For nuisance parameters affecting the normalisation of different processes, a log-normal probability density function is used. For uncertainties that also affect the shape, a Gaussian distribution is employed. The best fit value for μ is obtained by minimising the negative log likelihood function with respect to all the parameters. The Barlow-Beeston-lite method [88, 89] is employed to estimate the statistical uncertainties of the simulated samples. The maximum likelihood fit is implemented with the CMS statistical analysis tool COMBINE [90], which is based on the RooFit [91] and RooStats [92] frameworks.

6 Methodology for the differential measurements

Differential cross section measurements provide results that may be directly compared with theoretical predictions. The differential tW cross section is measured as a function of six observables without using information from the maximum likelihood fit of the inclusive measurement.

The collected data are affected by detector effects and are classified as detector level. Then, the parton level is defined by the particles produced after the generation of the hard-scattering process. When the information from the PS and hadronisation simulations is incorporated, this provides the particle level. The particle-level object definitions are summarised in table 1. These objects are constructed using stable generated particles (i.e.

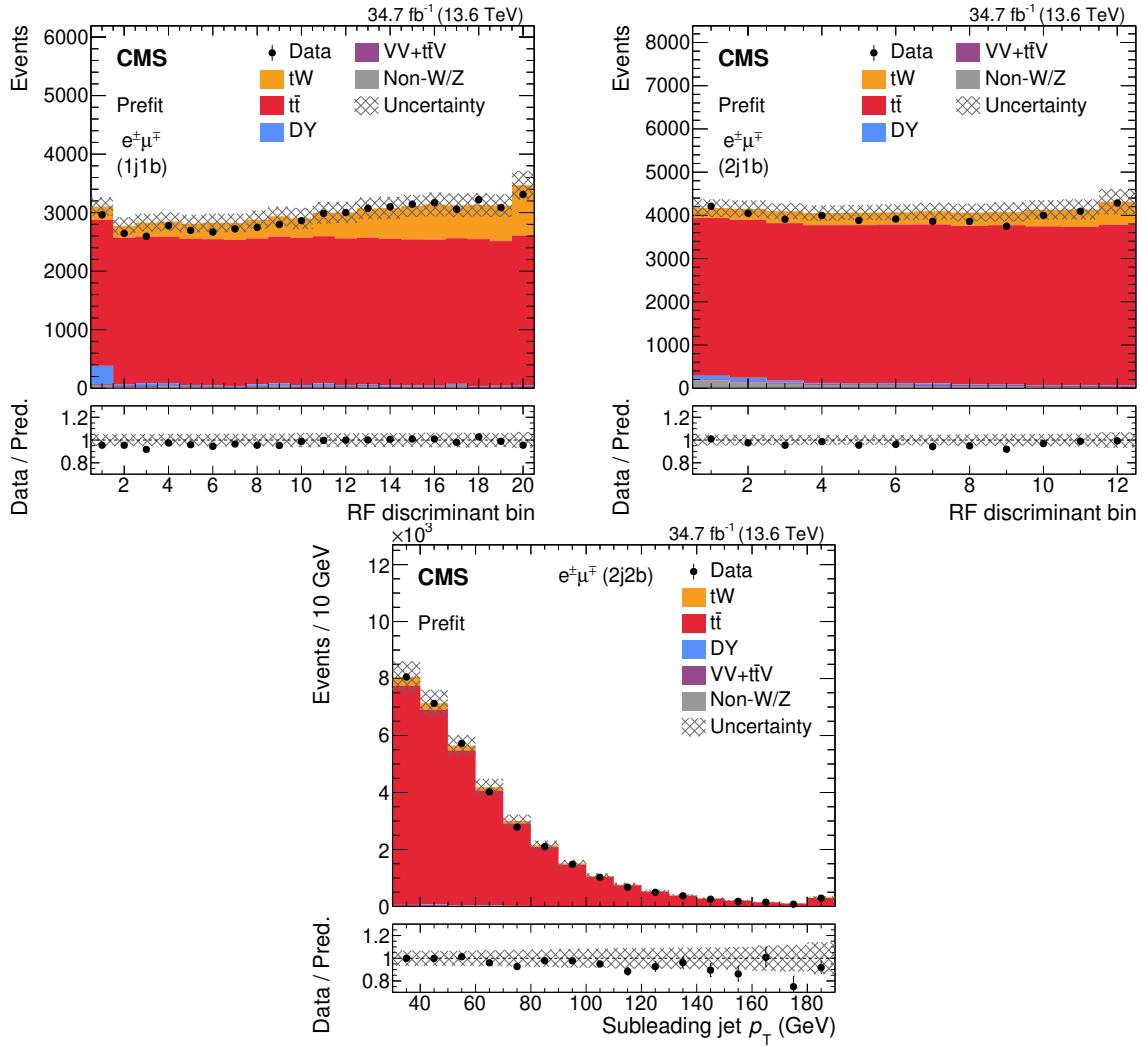


Figure 5. The distributions of the RF outputs for events in the $1j1b$ (upper left) and $2j1b$ (upper right) regions, and the subleading jet p_T for the $2j2b$ region (lower). The number of observed events (points) and estimated signal and background events (filled histograms) before the maximum likelihood fit are shown. The last bin of the subleading jet p_T distribution includes the overflow events. The vertical bars on the points represent the statistical uncertainty in the data, and the hatched band the total uncertainty in the estimated events before the fit. The lower panels display the ratio of the data to the sum of the estimated events (points) before the fit, with the bands giving the corresponding uncertainties.

with a lifetime larger than 30 ps), as described in ref. [93]. Electrons and muons not coming from hadronic decays (prompt leptons) are “dressed” by taking into account the momenta of nearby photons within a $\Delta R < 0.1$ cone, improving their momentum resolution. Jets are clustered from all of the stable particles excluding prompt muons, prompt electrons, prompt photons, and neutrinos, using the anti- k_T algorithm with a distance parameter of $R = 0.4$. The jet flavour is determined by the ghost-matching procedure [94]. For each b hadron, an additional collinear four-vector of infinitesimal magnitude is included in the jet clustering, and each jet that includes such a “ghost” is identified as a bottom jet. With these criteria, a fiducial region is defined as described in table 2. Requiring exactly one b jet reduces

Object	p_T (GeV)	$ \eta $
Muons	>20	<2.4
Electrons	>20	<2.4, excluding [1.444–1.566]
Jets	>30	<2.4
Loose jets	[20, 30]	<2.4

Table 1. Selection requirements for particle-level objects.

Observable	Requirement
Number of leptons	≥ 2
Leading lepton p_T	>25 GeV
Invariant mass of all dilepton pairs	>20 GeV
Number of jets	1
Number of loose jets	0
Number of b jets	1

Table 2. Definition of the fiducial region.

the potential to have events from the doubly-resonant diagrams (see figure 2), reducing the contribution from $t\bar{t}$ production and providing a purer signal region that is less affected by the systematic uncertainties associated with the $t\bar{t}$ background process. The interference effects, and the differences between the various models used to treat it, are expected to be higher when the presence of events from doubly-resonant diagrams is larger. Therefore, this choice of fiducial region reduces these effects and the accompanying modelling uncertainty associated with the interference treatment (as discussed in section 7).

Unfolding techniques [95] are used to determine the distributions without the detector effects, unrolling from the detector level to particle level. Unfolding to the particle level instead of unfolding to the parton level is chosen due to the reduction of the migration and efficiency corrections, and because this allows for the fiducial region definition to be in close correspondence with the event selection of the analysis. For each measured observable, the response matrix (R) parameterising the efficiency and the migrations among bins is constructed using the signal MC simulations. The number of signal events in the bins of the unfolded distribution ($N_j^{\text{sig},\text{unf}}$) can be estimated solving the equation

$$N_i^{\text{sig}} = N_i - N_i^{\text{bkg}} = \sum_{j=1}^{n^{\text{unf}}} R_{ij} N_j^{\text{sig},\text{unf}}, \quad (6.1)$$

where N_i^{sig} is the number of signal events in bin i at the detector level, N_i is the number of observed events in bin i , N_i^{bkg} is the number of expected background events in the same bin, and n^{unf} is the total number of bins in the unfolded distribution. Signal events falling outside the fiducial region are considered as an additional background. In order to obtain the number of events after unfolding, a χ^2 minimisation is performed to solve eq. (6.1). In this paper, the equation is solved using the implementation of TUNFOLD [96]. If needed, regularisation terms

could be added to the χ^2 function in order to suppress unphysical fluctuations. All response matrices obtained in this analysis exhibit condition numbers ≤ 7 and are thus considered well-conditioned and suitable for unfolding without regularisation. The condition number is computed as the ratio between the largest and smallest singular value of the matrix.

The differential cross section is measured as a function of the following physical observables:

- leading lepton p_T .
- jet p_T .
- $\Delta\varphi(e^\pm, \mu^\mp)$: the azimuthal angle difference between the two leptons.
- $p_z(e^\pm, \mu^\mp, j)$: the longitudinal momentum component of the dilepton+jet system.
- $m(e^\pm, \mu^\mp, j)$: the invariant mass of the dilepton+jet system.
- $m_T(e^\pm, \mu^\mp, j, \vec{p}_T^{\text{miss}})$: the transverse mass of the dilepton+jet+ \vec{p}_T^{miss} system. For a collection of particles with $\vec{p}_{T,i}$, m_T is defined as:

$$m_T = \sqrt{\left(\sum_i |\vec{p}_{T,i}|\right)^2 - \left|\sum_i \vec{p}_{T,i}\right|^2}. \quad (6.2)$$

The first two variables provide information on the kinematic properties of the events. The $\Delta\varphi(e^\pm, \mu^\mp)$ variable probes the kinematic and polarisation correlations between the W boson and the top quark. The $p_z(e^\pm, \mu^\mp, j)$ distribution can be used to study the boost of the tW system. The last two variables, the dilepton+jet invariant mass and m_T , are sensitive to the invariant mass of the tW system. The distributions from the data and simulation for these variables in the signal region, 1j1b with zero loose jets, are shown in figure 6. Overall, a good agreement between the data and prediction is observed within the uncertainties.

After the unfolding, the result is normalised to the fiducial cross section (obtained from the sum of contents of the bins) and the bin width. The uncertainties are propagated taking into account the correlations between the uncertainties from the differential cross section and the fiducial cross section. The Asimov data set [97] has been used to verify the performance and the closure of the unfolding procedure.

7 Systematic uncertainties

Apart from statistical uncertainties, the determination of both inclusive and differential tW cross sections is influenced by systematic uncertainties stemming from detector effects and theoretical assumptions. Each source of systematic uncertainty is assessed individually through appropriate variations of simulations or parameter values in the analysis within their estimated uncertainties. These systematic uncertainties are integrated into the maximum likelihood fit of the inclusive measurement as nuisance parameters. For the differential measurements, the effect of every uncertainty source is considered in both the response matrices and signal extraction. Signal events falling outside the fiducial region are considered as background and are subtracted from the data during the signal extraction. The impact

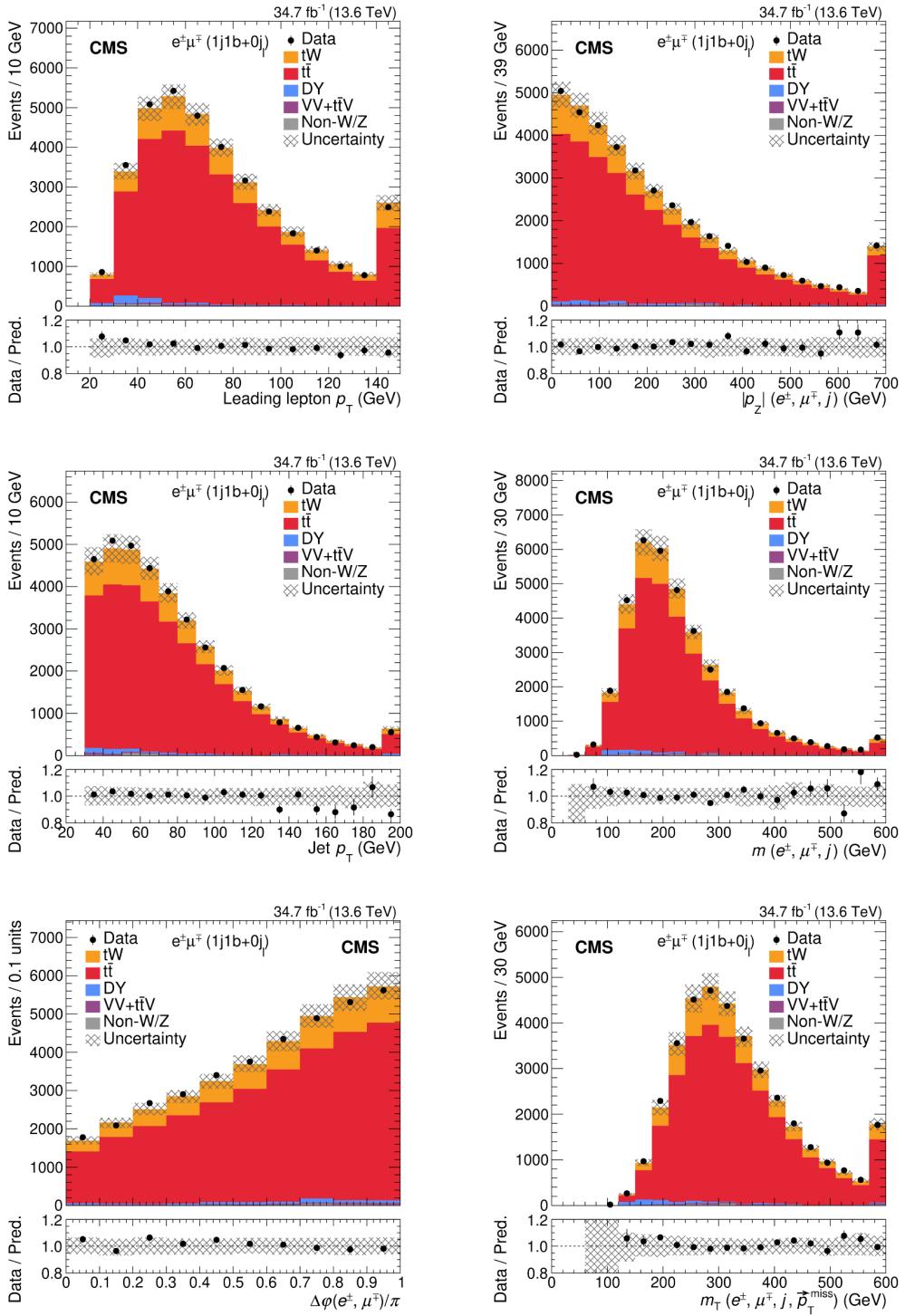


Figure 6. The measured distributions from data (points) and MC simulations (filled histograms) before the maximum likelihood fit of the six observables used to measure the tW differential cross sections. Signal events in the $1j1b$ region with 0 loose jets ($0j_1$) are selected. The last bin of each distribution contains the overflow events. The vertical bars on the data show the statistical uncertainty. The hatched band displays the sum of the statistical and systematic uncertainties in the MC predictions. The lower panels show the ratio of the data to the sum of the MC expectations.

of each uncertainty source on the unfolded results is determined by repeating the unfolding with variations corresponding to each source.

In instances where the statistical uncertainty of a systematic variation is comparable to or larger than the size of the systematic variation or where there is significant bin-to-bin variation, smoothing of the systematic templates is required. To achieve this, a lowess-based smoothing algorithm [98] is employed, which effectively constrains the shape differences between the upward and downward fluctuations.

The following subsections outline the sources considered for both the inclusive and differential measurements. All experimental uncertainty sources are considered for all processes, whereas modelling uncertainties are only considered for the tW and $t\bar{t}$ processes. Since data and simulation samples from different periods (before and after the ECAL water leak) are considered, it is specified whether each uncertainty is correlated across these two periods or not. In the case of modelling uncertainties, it is indicated whether they are correlated among processes or not.

7.1 Experimental uncertainties

JES and JER: The uncertainty is determined by varying the jet p_T scale and resolution within the uncertainties in bins of jet p_T and η , as described in ref. [50]. The JES uncertainty sources are propagated to \vec{p}_T^{miss} and separated into various components that are correlated or uncorrelated across periods in different groups. More details about the JES groups can be found in the caption of figure 9. The JER uncertainty is considered uncorrelated across data-taking periods, one component for each.

Unclustered energy: The influence of unclustered energy from the calorimeters on \vec{p}_T^{miss} is taken into account by considering the momentum resolution of the diverse PF candidates [44, 99, 100]. This uncertainty is considered uncorrelated across periods.

b tagging: The uncertainties arising from the b tagging data-to-simulation scale factors (SFs) are evaluated by varying them, within their uncertainties, for b, c, light-flavoured, and gluon jets. For heavy-flavour (b and c) quarks, these uncertainties are split into one correlated source across periods that includes the systematic part of the uncertainty and two uncorrelated sources that include the statistical part. For light-flavoured/gluon jet misidentification cases, one correlated source that includes both parts is used.

Trigger and lepton identification: The uncertainties associated with the trigger efficiency, and lepton ID, reconstruction (for electrons), and isolation are estimated by varying the data-to-simulation SFs according to their uncertainties. Trigger uncertainties contain statistical sources (from both the MC simulations and data used) and systematic sources that estimate the impact of the event topology used for their derivation. Lepton ID and isolation SFs are determined via the tag-and-probe method [101] as a function of the lepton p_T and η . For muons (electrons), an additional uncertainty of 0.5 (1)% is added in quadrature to account for the extrapolation from the phase space in which the isolation SFs are measured and the phase space for the analysis. The ID and isolation uncertainties of muons are considered separately. The muon ID and isolation uncertainties are split into statistical and systematic sources. For electrons, the ID

uncertainties also contain isolation. The trigger and the statistical component of the muon ID and isolation uncertainties are uncorrelated across periods while the other mentioned sources are considered correlated.

Electron scale and resolution: To account for the uncertainties in the electron momentum scale and resolution, the momenta of the electrons are varied within the uncertainties. These effects are uncorrelated across periods.

Pileup: The uncertainty attributed to the number of pileup interactions in simulation is derived by varying the total inelastic pp cross section of 69.2 mb [102] within its uncertainty of 4.6%. This uncertainty is correlated across the two periods.

Luminosity: The uncertainty in the integrated luminosity is estimated to be 1.4% for 2022 [103, 104], and is correlated across the periods.

7.2 Modelling uncertainties

To evaluate the impact of theoretical assumptions in the modelling, the analysis is repeated while replacing the standard POWHEG BOX+PYTHIA8 tW or tt} simulation with dedicated simulation samples using modified parameters, or by reweighting the nominal samples. Each modelling uncertainty source is considered correlated across periods.

ME scales: The uncertainty in the modelling of the hard process is considered for tW and tt} events and is determined by changing independently the μ_R and μ_F scales in the simulation samples by factors of 2 and 0.5 relative to their common nominal value. This uncertainty is considered separately for tW and tt} events.

PS: To take into account the PS uncertainties, different effects are considered:

- Underlying event: PYTHIA parameters are tuned to match measurements of the underlying event [63, 105]. These account for nonperturbative QCD effects. They are varied up and down in simulated tW and tt} events. This variation is correlated between tW and tt} events.
- ME/PS matching: the uncertainty in the combination of the ME calculation with the PS in simulated tt} events is estimated from the variation of the POWHEG parameter h_{damp} , which regulates the damping of real emissions in the NLO calculation when matching to the PS [105]. The nominal value used for the h_{damp} parameter (250 GeV) [56] is taken as the rounded average of the values used by the ATLAS (258.75 GeV) and CMS (237.8775 GeV) [63] Collaborations. For the variations (158 and 418 GeV), they are obtained performing a translation of the old values (150.7305, 237.8775, and 397.6125 GeV) [63]. This variation is only considered for tt} events.
- Initial- and final-state radiation scales: the PS scale considered for simulating the initial- and final-state radiations is varied up and down by a factor of two and only considered for tW and tt} events. These variations are motivated by the uncertainties in the PS tuning [105]. This variation is performed separately for

tW and $t\bar{t}$ events in the case of the initial-state radiation, and together for the final-state radiation.

- Colour reconnection: the modelling of colour reconnection has been studied in ref. [106]. A simulation including colour reconnection of early resonance decays is used as the reference model. The uncertainties that arise from ambiguities in modelling are estimated by comparing with two alternative models of colour reconnection: a model with string formation beyond leading colour, and a model in which the gluons can be moved to another string [107]. All models are tuned to measurements of the underlying event [105, 108]. The different models are used to define separate variations in treating this uncertainty. This variation is correlated between tW and $t\bar{t}$ events.

PDF and α_S : The uncertainty arising from the choice of PDFs is assessed by reweighting the simulated tW and $t\bar{t}$ events according to the 100 NNPDF3.1 replicas [61]. As they represent the contents of a diagonalised Hessian matrix, the eigenvectors are summed quadratically to obtain the PDF uncertainty. On the other hand, the uncertainty in the value of α_S used in the PDFs is considered separately. These uncertainties are correlated between tW and $t\bar{t}$ events.

Top quark mass: The nominal m_t of 172.5 GeV is modified by ± 3 GeV in the simulation. In order to assess a more realistic uncertainty based on current experimental precision, a variation of ± 0.33 GeV, corresponding to the uncertainty in the measurement of m_t from the CMS and ATLAS experiments [109], is applied and obtained assuming linearity of the deviations from the nominal value. The difference with respect to the nominal results is taken as the uncertainty and is considered for tW and $t\bar{t}$ events. This variation is correlated between tW and $t\bar{t}$ events.

Top quark p_T : Previous measurements of the differential cross section for $t\bar{t}$ production have indicated that the top quark exhibits a lower average p_T value compared to predictions from the POWHEG BOX simulation [110–112]. This is understood and considered to be an effect of missing higher-order calculations. To address this, SFs are derived by comparing the generated distributions of the top quark p_T at NNLO pQCD accuracy including NLO electroweak corrections [113] with the NLO pQCD POWHEG BOX calculations at 13 TeV. Additional SFs are derived to extrapolate these SFs to 13.6 TeV. The nominal $t\bar{t}$ events are corrected with these SFs and the difference between corrected and uncorrected shapes is taken as the uncertainty associated with the modelling of the top quark p_T . This uncertainty is symmetrised, with the up variation corresponding to the unweighted template and the down variation to the symmetrised template going in the opposite direction. This variation only affects $t\bar{t}$ events.

DR/DS methods: The difference between the DR and DS methods is used to estimate the uncertainties in the tW simulation.

Process	1j1b	2j1b	2j2b
tW	$8\,000 \pm 300$	$3\,660 \pm 160$	$1\,140 \pm 70$
t̄t	$49\,200 \pm 300$	$42\,520 \pm 190$	$33\,380 \pm 160$
Drell-Yan	670 ± 60	330 ± 40	42 ± 7
VV+t̄tV	460 ± 50	450 ± 70	190 ± 30
Non-W/Z	340 ± 70	810 ± 50	64 ± 12
Total	$58\,700 \pm 150$	$47\,780 \pm 130$	$34\,810 \pm 130$
Observed	58 635	47 810	34 818

Table 3. The number of estimated signal and background events after the fit in the 1j1b, 2j1b, and 2j2b regions compared to the observed number of events. The total uncertainties in the estimated events after the fit are given.

7.3 Background normalisation uncertainties

An uncertainty of 3.5%, taken from the total uncertainty of the experimental measurement of the t̄t inclusive cross section at $\sqrt{s} = 13.6$ TeV [13], is included as the uncertainty in the normalisation of the t̄t background. For the t̄tV and VV backgrounds, a normalisation uncertainty of 50% is used, as in ref. [27]. For the non-W/Z background contribution, a normalisation uncertainty of 15% is taken from an estimation performed with data in a region where the selected leptons have the same electric charge. The DY background is assigned a 10% normalisation uncertainty based on the differences observed between data and simulation in regions of phase space closely resembling the signal region.

8 Results

8.1 Inclusive measurement

The measured signal strength, $\mu = \sigma_{\text{tW}}/\sigma_{\text{tW}}^{\text{SM}}$, is obtained by maximising the likelihood function with respect to all its parameters. The fit is performed using the RF discriminants in the 1j1b and 2j1b regions and the subleading jet p_T distribution in the 2j2b region. These distributions, after the fit to the data, are shown in figure 7. An improved agreement between the data and the estimated events after the maximum likelihood fit is observed compared to the distributions before the fit shown in figure 5. The number of observed and estimated signal and background event yields in the three regions after the fit are also given in table 3. The signal strength result corresponds to a measured tW inclusive cross section of

$$\sigma_{\text{tW}} = 82.3 \pm 2.1 \text{ (stat)} {}^{+9.9}_{-9.7} \text{ (syst)} \pm 3.3 \text{ (lumi)} \text{ pb}, \quad (8.1)$$

that is consistent with the SM expectation of $87.9 {}^{+2.0}_{-1.9}$ (scale) ± 2.4 (PDF+ α_S) pb.

The result from this measurement is shown in figure 8 together with other measurements from the CMS Collaboration at different centre-of-mass energies, along with a global comparison to the SM prediction.

Figure 9 shows the twenty largest impacts on the signal strength and the corresponding nuisance parameters. The impact is defined as the shift $\Delta\hat{\mu}$ induced in μ when the

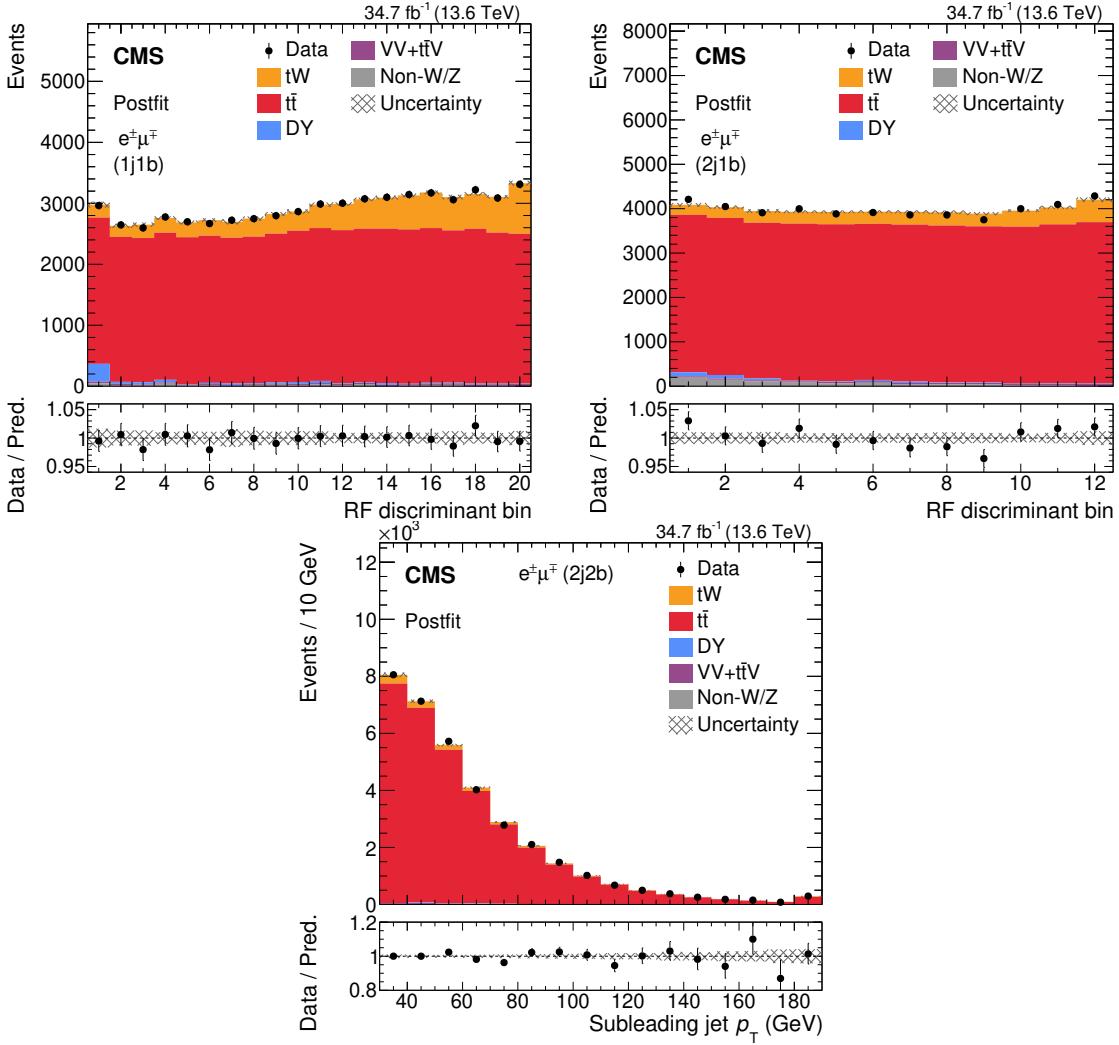


Figure 7. The distributions of the RF outputs for events in the 1j1b (upper left) and 2j1b (upper right) regions, and the subleading jet p_T for the 2j2b region (lower). The number of observed events (points) and estimated signal and background events (filled histograms) from the maximum likelihood fit are shown. The last bin of the subleading jet p_T distribution includes the overflow events. The vertical bars on the points represent the statistical uncertainty in the data, and the hatched band the total uncertainty in the estimated events after the fit. The lower panels display the ratio of the data to the sum of the estimated events (points) after the fit, with the bands giving the corresponding uncertainties.

nuisance parameter θ is varied by ± 1 standard deviation around its best fit value. The leading uncertainties are from the JES corrections, top quark p_T modelling, underlying event description, and b tagging efficiencies. Figure 9 also shows the fit constraints of the nuisance parameters, $(\hat{\theta} - \theta_0)/\Delta\theta$, where $\hat{\theta}$ and θ_0 are the values after and before the fit of the nuisance parameter θ , and $\Delta\theta$ the corresponding uncertainty before the fit. The uncertainty coming from the b tagging efficiency is less constrained and the DY normalisation uncertainty has less impact than in ref. [27].

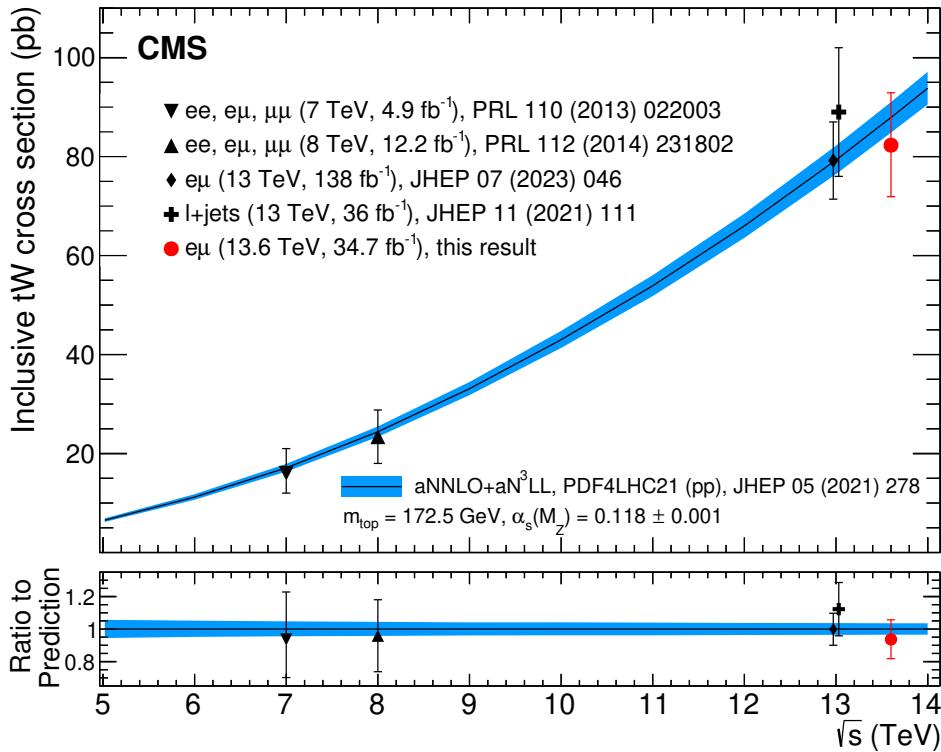


Figure 8. The tW cross section as a function of \sqrt{s} , as obtained in this analysis (red filled circle) and in previous measurements by the CMS experiment [4, 22, 27, 30] (black markers), with vertical bars on the markers indicating the total uncertainty in the measurements. Points corresponding to measurements at the same \sqrt{s} are horizontally shifted for better visibility. The SM prediction [15–17] is shown with a black line and blue uncertainty bands.

8.2 Normalised fiducial differential cross section measurements

The tW differential cross sections, normalised to the bin width and the total fiducial cross section $\sigma_{\text{fid.}}$, which is obtained by summing the contents of the particle-level bins, are shown in figure 10 for the data and the simulation predictions. The uncertainties, roughly 20–40% in most cases, depending on the distributions and bins, are dominated by the statistical uncertainties. Tables 4 and 5 give the p -values from the χ^2 goodness-of-fit tests done for the distributions, using the different MC generators and taking into account the full covariance matrix of each result, as well as the statistical uncertainties of the predictions. The full covariance matrix is derived by normalising the covariance matrix to the measured fiducial cross section and bin width. The p -values indicate good agreement between data and all MC predictions in the six observables. The methods to treat the interference between tW and t \bar{t} , DR, DR2, DS, and DS with a dynamic factor, show small differences among them, pointing to small interference effects on these distributions in the defined fiducial region. This is also true for the DR predictions interfaced with HERWIG7. The smallest p -values are obtained for the $\Delta\varphi(e^\pm, \mu^\mp)$ differential cross section, consistent with a similar result reported by CMS in ref. [115].

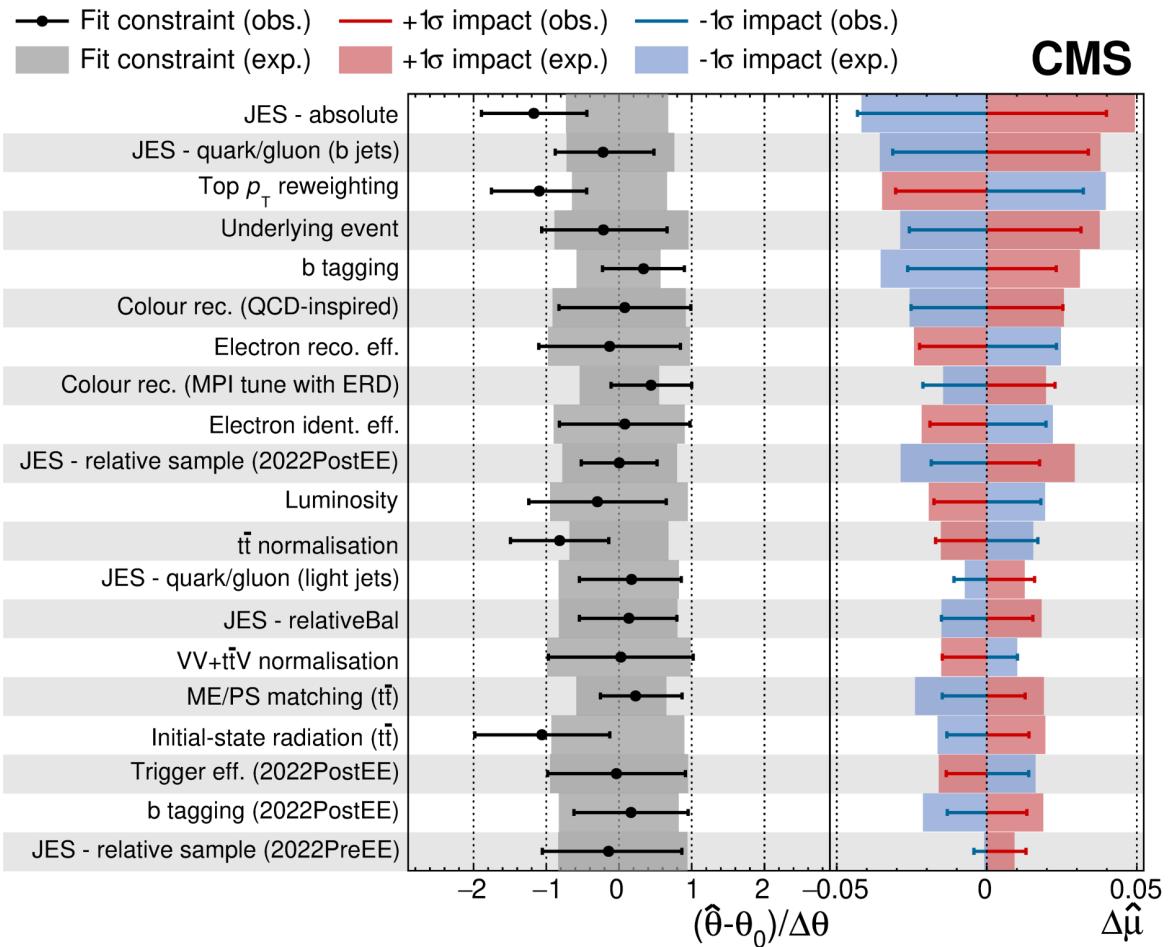


Figure 9. The twenty largest impacts $\Delta\hat{\mu}$ (right column) and fit constraints $(\hat{\theta} - \theta_0)/\Delta\theta$ (middle column) of the nuisance parameters listed in the left column from the maximum likelihood fit used to determine the inclusive tW cross section. The horizontal bars on the fit constraints show the ratio of the uncertainties of the fit result to the previous ones, effectively giving the constraint on the nuisance parameter. If the period is specified alongside the uncertainty name, it indicates that this is the component of the uncertainty uncorrelated by periods. There are two possible periods, before (2022PreEE) and after (2022PostEE) ECAL water leak. The JES uncertainties are divided into several sources, where “JES — absolute” groups contributions from scale corrections in the barrel, pileup corrections, and initial- and final-state radiation corrections; “JES — relative sample” encodes the uncertainty in the η -dependent calibration of the jets; “JES — relativeBal” accounts for the full difference between log-linear fits of MPF (Missing transverse energy Projection Fraction) and p_T balance methods [114]; and “JES — quark/gluon” comes from the corrections applied to correct the different detector response to gluon and quark jets. This last uncertainty is split in three components. These components are: light for the gluon and up, down, and strange quark jets, charm for the c jets, and bottom for the b jets.

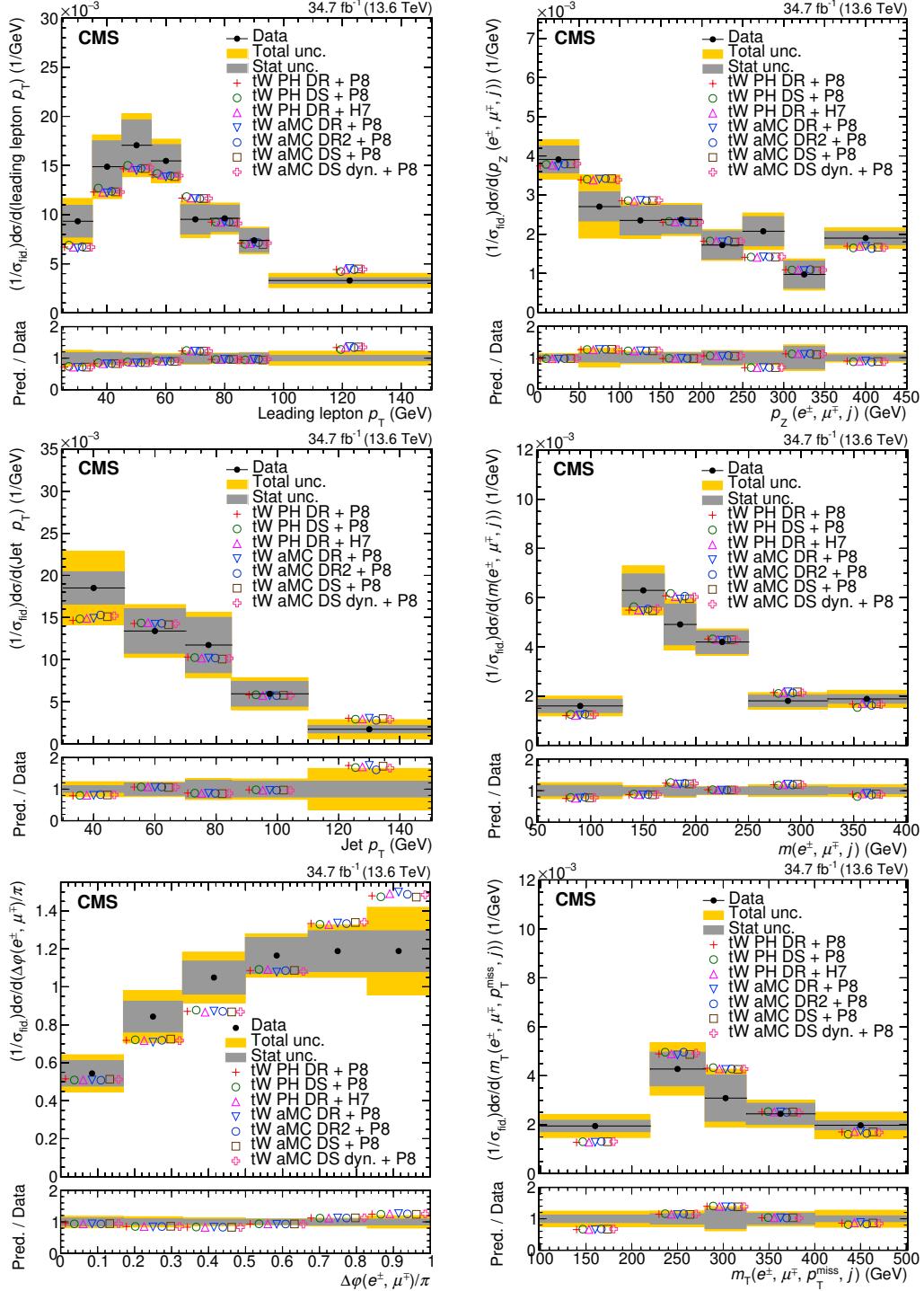


Figure 10. Normalised fiducial differential tW production cross sections as functions of the p_T of the leading lepton (upper left), $p_z(e^\pm, \mu^\mp, j)$ (upper right), p_T of the jet (middle left), $m(e^\pm, \mu^\mp, j)$ (middle right), $\Delta\varphi(e^\pm, \mu^\mp)$ (lower left), and $m_T(e^\pm, \mu^\mp, j, p_T^{\text{miss}})$ (lower right). The horizontal bars on the points show the bin width. Predictions from POWHEG BOX (PH) DR and DS + PYTHIA8 (P8), POWHEG BOX DR + HERWIG7 (H7), MADGRAPH5_aMC@NLO (aMC) DR, DR2, DS, and DS with a dynamic factor + PYTHIA8 are also shown. The grey band represents the statistical uncertainty and the yellow band the total uncertainty. In the lower panels, the ratio of the predictions to the data is shown.

Variable	PH DR + P8	PH DS + P8	PH DR + H7
Leading lepton p_T	0.92	0.94	0.92
Jet p_T	0.93	0.98	0.94
$\Delta\varphi(e^\pm, \mu^\mp)/\pi$	0.79	0.83	0.77
$p_z(e^\pm, \mu^\mp, j)$	0.86	0.88	0.85
$m_T(e^\pm, \mu^\mp, j, \vec{p}_T^{\text{miss}})$	0.93	0.96	0.93
$m(e^\pm, \mu^\mp, j)$	0.88	0.74	0.92

Table 4. The p -values from the χ^2 goodness-of-fit tests comparing the six differential cross section measurements with the predictions from POWHEG BOX (PH) DR and DS + PYTHIA8 (P8) and POWHEG BOX DR + HERWIG7 (H7). The complete covariance matrix from the results and the statistical uncertainties in the predictions are taken into account.

Variable	aMC DR + P8	aMC DR2 + P8	aMC DS + P8	aMC DS dyn. + P8
Leading lepton p_T	0.91	0.95	0.92	0.93
Jet p_T	0.91	0.93	0.94	0.98
$\Delta\varphi(e^\pm, \mu^\mp)/\pi$	0.75	0.79	0.79	0.76
$p_z(e^\pm, \mu^\mp, j)$	0.89	0.86	0.86	0.85
$m_T(e^\pm, \mu^\mp, j, \vec{p}_T^{\text{miss}})$	0.92	0.96	0.94	0.95
$m(e^\pm, \mu^\mp, j)$	0.98	0.88	0.94	0.93

Table 5. The p -values from the χ^2 goodness-of-fit tests comparing the six differential cross section measurements with the predictions from MADGRAPH5_aMC@NLO (aMC) DR, DR2, DS, and DS with a dynamic factor + PYTHIA8. The complete covariance matrix from the results and the statistical uncertainties in the predictions are taken into account.

9 Summary

Inclusive and normalised differential cross sections of top quark production in association with a W boson are measured in proton-proton collision data at $\sqrt{s} = 13.6$ TeV. The selected data, corresponding to an integrated luminosity of 34.7 fb^{-1} , contain events with an electron and a muon of opposite charge.

For the inclusive measurement, the events have been categorised depending on the number of jets and jets originating from the fragmentation of bottom quarks. The signal is measured using a maximum likelihood fit to the distribution of random forest discriminants in the regions with one or two jets where one of them is identified as originating from the fragmentation of a bottom quark (b jet), and to the transverse momentum (p_T) distribution of the second-highest p_T jet in a third category with two jets, both of which are b jets. The measured inclusive cross section is $82.3 \pm 2.1 \text{ (stat)}^{+9.9}_{-9.7} \text{ (syst)} \pm 3.3 \text{ (lumi)} \text{ pb}$, with a total relative uncertainty of about 13%. This measurement is in agreement with the latest theoretical prediction at approximate next-to-next-to-next-to-leading order accuracy in perturbative quantum chromodynamics and with other measurements.

The differential cross section measurements are performed as functions of six kinematic observables of the events in the fiducial phase space corresponding to the selection criteria.

The results have relative uncertainties in the range of 20–40%, depending on the measured observable. The uncertainties are mainly statistical. There is good agreement between the measurements and the predictions from the different event generators. The different approaches used to simulate tW events give similar values in all distributions, which points to small effects related to the $tW/t\bar{t}$ interference on these distributions in the defined fiducial region.

Acknowledgments

We congratulate our colleagues in the CERN accelerator departments for the excellent performance of the LHC and thank the technical and administrative staffs at CERN and at other CMS institutes for their contributions to the success of the CMS effort. In addition, we gratefully acknowledge the computing centres and personnel of the Worldwide LHC Computing Grid and other centres for delivering so effectively the computing infrastructure essential to our analyses. Finally, we acknowledge the enduring support for the construction and operation of the LHC, the CMS detector, and the supporting computing infrastructure provided by the following funding agencies: SC (Armenia), BMBWF and FWF (Austria); FNRS and FWO (Belgium); CNPq, CAPES, FAPERJ, FAPERGS, and FAPESP (Brazil); MES and BNSF (Bulgaria); CERN; CAS, MoST, and NSFC (China); MINCIENCIAS (Colombia); MSES and CSF (Croatia); RIF (Cyprus); SENESCYT (Ecuador); ERC PRG, RVTT3 and MoER TK202 (Estonia); Academy of Finland, MEC, and HIP (Finland); CEA and CNRS/IN2P3 (France); SRNSF (Georgia); BMBF, DFG, and HGF (Germany); GSRI (Greece); NKFIH (Hungary); DAE and DST (India); IPM (Iran); SFI (Ireland); INFN (Italy); MSIP and NRF (Republic of Korea); MES (Latvia); LMTLT (Lithuania); MOE and UM (Malaysia); BUAP, CINVESTAV, CONACYT, LNS, SEP, and UASLP-FAI (Mexico); MOS (Montenegro); MBIE (New Zealand); PAEC (Pakistan); MES and NSC (Poland); FCT (Portugal); MESTD (Serbia); MCIN/AEI and PCTI (Spain); MOSTR (Sri Lanka); Swiss Funding Agencies (Switzerland); MST (Taipei); MHESI and NSTDA (Thailand); TUBITAK and TENMAK (Turkey); NASU (Ukraine); STFC (United Kingdom); DOE and NSF (U.S.A.).

Individuals have received support from the Marie-Curie programme and the European Research Council and Horizon 2020 Grant, contract Nos. 675440, 724704, 752730, 758316, 765710, 824093, 101115353, 101002207, and COST Action CA16108 (European Union); the Leventis Foundation; the Alfred P. Sloan Foundation; the Alexander von Humboldt Foundation; the Science Committee, project no. 22rl-037 (Armenia); the Belgian Federal Science Policy Office; the Fonds pour la Formation à la Recherche dans l’Industrie et dans l’Agriculture (FRIA-Belgium); the F.R.S.-FNRS and FWO (Belgium) under the “Excellence of Science — EOS” — be.h project n. 30820817; the Beijing Municipal Science & Technology Commission, No. Z191100007219010 and Fundamental Research Funds for the Central Universities (China); the Ministry of Education, Youth and Sports (MEYS) of the Czech Republic; the Shota Rustaveli National Science Foundation, grant FR-22-985 (Georgia); the Deutsche Forschungsgemeinschaft (DFG), among others, under Germany’s Excellence Strategy — EXC 2121 “Quantum Universe” — 390833306, and under project number 400140256 — GRK2497; the Hellenic Foundation for Research and Innovation (HFRI), Project Number 2288 (Greece); the Hungarian Academy of Sciences, the New National

Excellence Program — ÚNKP, the NKFIH research grants K 131991, K 133046, K 138136, K 143460, K 143477, K 146913, K 146914, K 147048, 2020-2.2.1-ED-2021-00181, and TKP2021-NKTA-64 (Hungary); the Council of Science and Industrial Research, India; ICSC — National Research Centre for High Performance Computing, Big Data and Quantum Computing and FAIR — Future Artificial Intelligence Research, funded by the NextGenerationEU program (Italy); the Latvian Council of Science; the Ministry of Education and Science, project no. 2022/WK/14, and the National Science Center, contracts Opus 2021/41/B/ST2/01369 and 2021/43/B/ST2/01552 (Poland); the Fundação para a Ciência e a Tecnologia, grant CEECIND/01334/2018 (Portugal); the National Priorities Research Program by Qatar National Research Fund; MCIN/AEI/10.13039/501100011033, ERDF “a way of making Europe”, and the Programa Estatal de Fomento de la Investigación Científica y Técnica de Excelencia María de Maeztu, grant MDM-2017-0765 and Programa Severo Ochoa del Principado de Asturias (Spain); the Chulalongkorn Academic into Its 2nd Century Project Advancement Project, and the National Science, Research and Innovation Fund via the Program Management Unit for Human Resources & Institutional Development, Research and Innovation, grant B39G670016 (Thailand); the Kavli Foundation; the Nvidia Corporation; the SuperMicro Corporation; the Welch Foundation, contract C-1845; and the Weston Havens Foundation (U.S.A.).

Data Availability Statement. This article has associated data in a data repository. Release and preservation of data used by the CMS Collaboration as the basis for publications is guided by the [CMS data preservation, re-use, and open access policy](#).

Code Availability Statement. This article has associated code in a code repository. The CMS core software is publicly available on [GitHub](#).

Open Access. This article is distributed under the terms of the Creative Commons Attribution License ([CC-BY4.0](#)), which permits any use, distribution and reproduction in any medium, provided the original author(s) and source are credited.

References

- [1] A.S. Belyaev, E.E. Boos and L.V. Dudko, *Single top quark at future hadron colliders: complete signal and background study*, *Phys. Rev. D* **59** (1999) 075001 [[hep-ph/9806332](#)] [[INSPIRE](#)].
- [2] S. Frixione et al., *Single-top hadroproduction in association with a W boson*, *JHEP* **07** (2008) 029 [[arXiv:0805.3067](#)] [[INSPIRE](#)].
- [3] C.D. White, S. Frixione, E. Laenen and F. Maltoni, *Isolating Wt production at the LHC*, *JHEP* **11** (2009) 074 [[arXiv:0908.0631](#)] [[INSPIRE](#)].
- [4] CMS collaboration, *Observation of the associated production of a single top quark and a W boson in pp collisions at $\sqrt{s} = 8$ TeV*, *Phys. Rev. Lett.* **112** (2014) 231802 [[arXiv:1401.2942](#)] [[INSPIRE](#)].
- [5] W. Fang, B. Clerbaux, A. Giannmanco and R. Goldouzian, *Model-independent constraints on the CKM matrix elements $|V_{tb}|$, $|V_{ts}|$ and $|V_{td}|$* , *JHEP* **03** (2019) 022 [[arXiv:1807.07319](#)] [[INSPIRE](#)].

- [6] R. Rahaman and A. Subba, *Probing top quark anomalous moments in W boson associated single top quark production at the LHC using polarization and spin correlation*, *Phys. Rev. D* **108** (2023) 055027 [[arXiv:2306.06889](#)] [[INSPIRE](#)].
- [7] T.M.P. Tait and C.-P. Yuan, *Single top quark production as a window to physics beyond the standard model*, *Phys. Rev. D* **63** (2000) 014018 [[hep-ph/0007298](#)] [[INSPIRE](#)].
- [8] Q.-H. Cao, J. Wudka and C.-P. Yuan, *Search for new physics via single top production at the LHC*, *Phys. Lett. B* **658** (2007) 50 [[arXiv:0704.2809](#)] [[INSPIRE](#)].
- [9] V. Barger, M. McCaskey and G. Shaughnessy, *Single top and Higgs associated production at the LHC*, *Phys. Rev. D* **81** (2010) 034020 [[arXiv:0911.1556](#)] [[INSPIRE](#)].
- [10] D. Pinna, A. Zucchetta, M.R. Buckley and F. Canelli, *Single top quarks and dark matter*, *Phys. Rev. D* **96** (2017) 035031 [[arXiv:1701.05195](#)] [[INSPIRE](#)].
- [11] CMS collaboration, *Search for dark matter produced in association with a single top quark or a top quark pair in proton-proton collisions at $\sqrt{s} = 13$ TeV*, *JHEP* **03** (2019) 141 [[arXiv:1901.01553](#)] [[INSPIRE](#)].
- [12] ATLAS collaboration, *Search for dark matter produced in association with bottom or top quarks in $\sqrt{s} = 13$ TeV pp collisions with the ATLAS detector*, *Eur. Phys. J. C* **78** (2018) 18 [[arXiv:1710.11412](#)] [[INSPIRE](#)].
- [13] CMS collaboration, *First measurement of the top quark pair production cross section in proton-proton collisions at $\sqrt{s} = 13.6$ TeV*, *JHEP* **08** (2023) 204 [[arXiv:2303.10680](#)] [[INSPIRE](#)].
- [14] ATLAS collaboration, *Inclusive and differential cross-sections for dilepton $t\bar{t}$ production measured in $\sqrt{s} = 13$ TeV pp collisions with the ATLAS detector*, *JHEP* **07** (2023) 141 [[arXiv:2303.15340](#)] [[INSPIRE](#)].
- [15] N. Kidonakis and N. Yamanaka, *Higher-order corrections for tW production at high-energy hadron colliders*, *JHEP* **05** (2021) 278 [[arXiv:2102.11300](#)] [[INSPIRE](#)].
- [16] N. Kidonakis, *Two-loop soft anomalous dimensions for single top quark associated production with a W^- or H^-* , *Phys. Rev. D* **82** (2010) 054018 [[arXiv:1005.4451](#)] [[INSPIRE](#)].
- [17] N. Kidonakis, *Soft-gluon corrections for tW production at N^3LO* , *Phys. Rev. D* **96** (2017) 034014 [[arXiv:1612.06426](#)] [[INSPIRE](#)].
- [18] PDF4LHC WORKING GROUP collaboration, *The PDF4LHC21 combination of global PDF fits for the LHC Run III*, *J. Phys. G* **49** (2022) 080501 [[arXiv:2203.05506](#)] [[INSPIRE](#)].
- [19] D0 collaboration, *Observation of single top quark production*, *Phys. Rev. Lett.* **103** (2009) 092001 [[arXiv:0903.0850](#)] [[INSPIRE](#)].
- [20] CDF collaboration, *First observation of electroweak single top quark production*, *Phys. Rev. Lett.* **103** (2009) 092002 [[arXiv:0903.0885](#)] [[INSPIRE](#)].
- [21] ATLAS collaboration, *Evidence for the associated production of a W boson and a top quark in ATLAS at $\sqrt{s} = 7$ TeV*, *Phys. Lett. B* **716** (2012) 142 [[arXiv:1205.5764](#)] [[INSPIRE](#)].
- [22] CMS collaboration, *Evidence for associated production of a single top quark and W boson in pp collisions at $\sqrt{s} = 7$ TeV*, *Phys. Rev. Lett.* **110** (2013) 022003 [[arXiv:1209.3489](#)] [[INSPIRE](#)].
- [23] ATLAS collaboration, *Measurement of the production cross-section of a single top quark in association with a W boson at 8 TeV with the ATLAS experiment*, *JHEP* **01** (2016) 064 [[arXiv:1510.03752](#)] [[INSPIRE](#)].

- [24] ATLAS collaboration, *Measurement of the cross-section for producing a W boson in association with a single top quark in pp collisions at $\sqrt{s} = 13$ TeV with ATLAS*, *JHEP* **01** (2018) 063 [[arXiv:1612.07231](https://arxiv.org/abs/1612.07231)] [[INSPIRE](#)].
- [25] CMS collaboration, *Measurement of the production cross section for single top quarks in association with W bosons in proton-proton collisions at $\sqrt{s} = 13$ TeV*, *JHEP* **10** (2018) 117 [[arXiv:1805.07399](https://arxiv.org/abs/1805.07399)] [[INSPIRE](#)].
- [26] ATLAS collaboration, *Measurement of single top-quark production in association with a W boson in pp collisions at $\sqrt{s} = 13$ TeV with the ATLAS detector*, *Phys. Rev. D* **110** (2024) 072010 [[arXiv:2407.15594](https://arxiv.org/abs/2407.15594)] [[INSPIRE](#)].
- [27] CMS collaboration, *Measurement of inclusive and differential cross sections for single top quark production in association with a W boson in proton-proton collisions at $\sqrt{s} = 13$ TeV*, *JHEP* **07** (2023) 046 [[arXiv:2208.00924](https://arxiv.org/abs/2208.00924)] [[INSPIRE](#)].
- [28] ATLAS collaboration, *Measurement of differential cross-sections of a single top quark produced in association with a W boson at $\sqrt{s} = 13$ TeV with ATLAS*, *Eur. Phys. J. C* **78** (2018) 186 [[arXiv:1712.01602](https://arxiv.org/abs/1712.01602)] [[INSPIRE](#)].
- [29] ATLAS collaboration, *Probing the quantum interference between singly and doubly resonant top-quark production in pp collisions at $\sqrt{s} = 13$ TeV with the ATLAS detector*, *Phys. Rev. Lett.* **121** (2018) 152002 [[arXiv:1806.04667](https://arxiv.org/abs/1806.04667)] [[INSPIRE](#)].
- [30] CMS collaboration, *Observation of tW production in the single-lepton channel in pp collisions at $\sqrt{s} = 13$ TeV*, *JHEP* **11** (2021) 111 [[arXiv:2109.01706](https://arxiv.org/abs/2109.01706)] [[INSPIRE](#)].
- [31] ATLAS collaboration, *Measurement of single top-quark production in association with a W boson in the single-lepton channel at $\sqrt{s} = 8$ TeV with the ATLAS detector*, *Eur. Phys. J. C* **81** (2021) 720 [[arXiv:2007.01554](https://arxiv.org/abs/2007.01554)] [[INSPIRE](#)].
- [32] *HEPData record for this analysis*, <https://doi.org/10.17182/hepdata.150675>, (2024).
- [33] CMS collaboration, *The CMS experiment at the CERN LHC, 2008* *JINST* **3** S08004 [[INSPIRE](#)].
- [34] CMS collaboration, *Development of the CMS detector for the CERN LHC run 3, 2024* *JINST* **19** P05064 [[arXiv:2309.05466](https://arxiv.org/abs/2309.05466)] [[INSPIRE](#)].
- [35] CMS collaboration, *Performance of the CMS Level-1 trigger in proton-proton collisions at $\sqrt{s} = 13$ TeV, 2020* *JINST* **15** P10017 [[arXiv:2006.10165](https://arxiv.org/abs/2006.10165)] [[INSPIRE](#)].
- [36] CMS collaboration, *The CMS trigger system, 2017* *JINST* **12** P01020 [[arXiv:1609.02366](https://arxiv.org/abs/1609.02366)] [[INSPIRE](#)].
- [37] CMS collaboration, *Measurement of inclusive and differential cross sections for W^+W^- production in proton-proton collisions at $\sqrt{s} = 13.6$ TeV*, [arXiv:2406.05101](https://arxiv.org/abs/2406.05101) [[INSPIRE](#)].
- [38] J. Mans et al., *CMS technical design report for the phase 1 upgrade of the hadron calorimeter*, CERN-LHCC-2012-015, CERN, Geneva, Switzerland (2012).
- [39] CMS collaboration, *Performance of the CMS phase-1 pixel detector with run 3 data*, CMS-DP-2022-047, CERN, Geneva, Switzerland (2022).
- [40] CMS collaboration, *Commissioning CMS online reconstruction with GPUs*, CMS-DP-2023-004, CERN, Geneva, Switzerland (2022).
- [41] CMS collaboration, *Run 3 luminosity measurements with the pixel luminosity telescope*, *PoS ICHEP2022* (2022) 936 [[INSPIRE](#)].

- [42] CMS collaboration, *Upgraded CMS fast beam condition monitor for LHC run 3 online luminosity and beam induced background measurements*, *JACoW I BIC2022* (2022) 540 [[INSPIRE](#)].
- [43] CMS BRIL collaboration, *The pixel luminosity telescope: a detector for luminosity measurement at CMS using silicon pixel sensors*, *Eur. Phys. J. C* **83** (2023) 673 [[arXiv:2206.08870](#)] [[INSPIRE](#)].
- [44] CMS collaboration, *Particle-flow reconstruction and global event description with the CMS detector*, *2017 JINST* **12** P10003 [[arXiv:1706.04965](#)] [[INSPIRE](#)].
- [45] D. Contardo et al., *Technical proposal for the phase-II upgrade of the CMS detector*, CERN-LHCC-2015-010, CERN, Geneva, Switzerland (2015) [[DOI:10.17181/CERN.VU8I.D59J](#)] [[INSPIRE](#)].
- [46] M. Cacciari, G.P. Salam and G. Soyez, *The anti- k_t jet clustering algorithm*, *JHEP* **04** (2008) 063 [[arXiv:0802.1189](#)] [[INSPIRE](#)].
- [47] M. Cacciari, G.P. Salam and G. Soyez, *FastJet user manual*, *Eur. Phys. J. C* **72** (2012) 1896 [[arXiv:1111.6097](#)] [[INSPIRE](#)].
- [48] D. Bertolini, P. Harris, M. Low and N. Tran, *Pileup per particle identification*, *JHEP* **10** (2014) 059 [[arXiv:1407.6013](#)] [[INSPIRE](#)].
- [49] CMS collaboration, *Pileup mitigation at CMS in 13 TeV data*, *2020 JINST* **15** P09018 [[arXiv:2003.00503](#)] [[INSPIRE](#)].
- [50] CMS collaboration, *Jet energy scale and resolution in the CMS experiment in pp collisions at 8 TeV*, *2017 JINST* **12** P02014 [[arXiv:1607.03663](#)] [[INSPIRE](#)].
- [51] CMS collaboration, *Jet algorithms performance in 13 TeV data*, [CMS-PAS-JME-16-003](#), CERN, Geneva, Switzerland (2017).
- [52] CMS collaboration, *Jet energy scale and resolution measurements using prompt run 3 data collected by CMS in the first months of 2022 at 13.6 TeV*, [CMS-DP-2022-054](#), CERN, Geneva, Switzerland (2022).
- [53] S. Alioli, P. Nason, C. Oleari and E. Re, *A general framework for implementing NLO calculations in shower Monte Carlo programs: the POWHEG BOX*, *JHEP* **06** (2010) 043 [[arXiv:1002.2581](#)] [[INSPIRE](#)].
- [54] S. Frixione, P. Nason and C. Oleari, *Matching NLO QCD computations with parton shower simulations: the POWHEG method*, *JHEP* **11** (2007) 070 [[arXiv:0709.2092](#)] [[INSPIRE](#)].
- [55] P. Nason, *A new method for combining NLO QCD with shower Monte Carlo algorithms*, *JHEP* **11** (2004) 040 [[hep-ph/0409146](#)] [[INSPIRE](#)].
- [56] ATLAS and CMS collaborations, *Improved common $t\bar{t}$ Monte-Carlo settings for ATLAS and CMS*, [CMS-NOTE-2023-004](#), CERN, Geneva, Switzerland (2023).
- [57] T.M.P. Tait, *The tW^- mode of single top production*, *Phys. Rev. D* **61** (1999) 034001 [[hep-ph/9909352](#)] [[INSPIRE](#)].
- [58] J. Alwall et al., *The automated computation of tree-level and next-to-leading order differential cross sections, and their matching to parton shower simulations*, *JHEP* **07** (2014) 079 [[arXiv:1405.0301](#)] [[INSPIRE](#)].
- [59] F. Demartin et al., *tWH associated production at the LHC*, *Eur. Phys. J. C* **77** (2017) 34 [[arXiv:1607.05862](#)] [[INSPIRE](#)].

- [60] S. Frixione, P. Nason and G. Ridolfi, *A positive-weight next-to-leading-order Monte Carlo for heavy flavour hadroproduction*, *JHEP* **09** (2007) 126 [[arXiv:0707.3088](#)] [[INSPIRE](#)].
- [61] NNPDF collaboration, *Parton distributions from high-precision collider data*, *Eur. Phys. J. C* **77** (2017) 663 [[arXiv:1706.00428](#)] [[INSPIRE](#)].
- [62] C. Bierlich et al., *A comprehensive guide to the physics and usage of PYTHIA 8.3*, *SciPost Phys. Codeb.* **2022** (2022) 8 [[arXiv:2203.11601](#)] [[INSPIRE](#)].
- [63] CMS collaboration, *Extraction and validation of a new set of CMS PYTHIA8 tunes from underlying-event measurements*, *Eur. Phys. J. C* **80** (2020) 4 [[arXiv:1903.12179](#)] [[INSPIRE](#)].
- [64] M. Bähr et al., *Herwig++ physics and manual*, *Eur. Phys. J. C* **58** (2008) 639 [[arXiv:0803.0883](#)] [[INSPIRE](#)].
- [65] J. Bellm et al., *Herwig 7.0/Herwig++ 3.0 release note*, *Eur. Phys. J. C* **76** (2016) 196 [[arXiv:1512.01178](#)] [[INSPIRE](#)].
- [66] J. Bellm et al., *Herwig 7.1 release note*, [arXiv:1705.06919](#) [[INSPIRE](#)].
- [67] CMS collaboration, *Development and validation of HERWIG 7 tunes from CMS underlying-event measurements*, *Eur. Phys. J. C* **81** (2021) 312 [[arXiv:2011.03422](#)] [[INSPIRE](#)].
- [68] R. Frederix and S. Frixione, *Merging meets matching in MC@NLO*, *JHEP* **12** (2012) 061 [[arXiv:1209.6215](#)] [[INSPIRE](#)].
- [69] GEANT4 collaboration, *GEANT4 — a simulation toolkit*, *Nucl. Instrum. Meth. A* **506** (2003) 250 [[INSPIRE](#)].
- [70] Y. Li and F. Petriello, *Combining QCD and electroweak corrections to dilepton production in FEWZ*, *Phys. Rev. D* **86** (2012) 094034 [[arXiv:1208.5967](#)] [[INSPIRE](#)].
- [71] J.M. Campbell, R.K. Ellis and C. Williams, *Vector boson pair production at the LHC*, *JHEP* **07** (2011) 018 [[arXiv:1105.0020](#)] [[INSPIRE](#)].
- [72] M. Czakon, P. Fiedler and A. Mitov, *Total top-quark pair-production cross section at hadron colliders through $O(\alpha_S^4)$* , *Phys. Rev. Lett.* **110** (2013) 252004 [[arXiv:1303.6254](#)] [[INSPIRE](#)].
- [73] M. Czakon and A. Mitov, *Top++: a program for the calculation of the top-pair cross-section at hadron colliders*, *Comput. Phys. Commun.* **185** (2014) 2930 [[arXiv:1112.5675](#)] [[INSPIRE](#)].
- [74] CMS collaboration, *Electron and photon reconstruction and identification with the CMS experiment at the CERN LHC*, **2021 JINST** **16** P05014 [[arXiv:2012.06888](#)] [[INSPIRE](#)].
- [75] CMS collaboration, *Performance of the CMS muon detector and muon reconstruction with proton-proton collisions at $\sqrt{s} = 13$ TeV*, **2018 JINST** **13** P06015 [[arXiv:1804.04528](#)] [[INSPIRE](#)].
- [76] H. Qu, C. Li and S. Qian, *Particle transformer for jet tagging*, in *Proc. 39th International Conference on Machine Learning (ICML 2022)*, Baltimore, MD, U.S.A., 17–23 July 2022 [[arXiv:2202.03772](#)] [[INSPIRE](#)].
- [77] CMS collaboration, *Adversarial training for b-tagging algorithms in CMS*, **CMS-DP-2022-049**, CERN, Geneva, Switzerland (2022).
- [78] CMS collaboration, *Transformer models for heavy flavor jet identification*, **CMS-DP-2022-050**, CERN, Geneva, Switzerland (2022).
- [79] CMS collaboration, *Illustration of the performance of the CMS tracker and reconstruction on early Run 3 data, on the example of D^* meson reconstruction*, **CMS-DP-2022-024**, CERN, Geneva, Switzerland (2022).

- [80] CMS collaboration, *Update of the MTD physics case*, CMS-DP-2022-025, CERN, Geneva, Switzerland (2022).
- [81] CMS collaboration, *Identification of heavy-flavour jets with the CMS detector in pp collisions at 13 TeV*, 2018 *JINST* **13** P05011 [[arXiv:1712.07158](#)] [[INSPIRE](#)].
- [82] E. Bols et al., *Jet flavour classification using DeepJet*, 2020 *JINST* **15** P12012 [[arXiv:2008.10519](#)] [[INSPIRE](#)].
- [83] A. Prinzie and D. Van den Poel, *Random multiclass classification: generalizing random forests to random MNL and random NB*, in *Database and expert systems applications*, Springer, Berlin, Heidelberg, Germany (2007), p. 349–358 [[DOI:10.1007/978-3-540-74469-6_35](#)].
- [84] F. Pedregosa et al., *Scikit-learn: machine learning in Python*, *J. Machine Learning Res.* **12** (2011) 2825 [[arXiv:1201.0490](#)] [[INSPIRE](#)].
- [85] L. Breiman, J. Friedman, R.A. Olshen and C.J. Stone, *Classification and regression trees*, Chapman and Hall/CRC, Boca Raton, FL, U.S.A. (2017) [[DOI:10.1201/9781315139470](#)] [[INSPIRE](#)].
- [86] R. Cousins, *Generalization of chisquare goodness-of-fit test for binned data using saturated models, with application to histograms*, https://www.physics.ucla.edu/~cousins/stats/cousins_saturated.pdf (2013).
- [87] E. Gross and O. Vitells, *Trial factors for the look elsewhere effect in high energy physics*, *Eur. Phys. J. C* **70** (2010) 525 [[arXiv:1005.1891](#)] [[INSPIRE](#)].
- [88] R.J. Barlow and C. Beeston, *Fitting using finite Monte Carlo samples*, *Comput. Phys. Commun.* **77** (1993) 219 [[INSPIRE](#)].
- [89] J.S. Conway, *Incorporating nuisance parameters in likelihoods for multisource spectra*, in the proceedings of the *PHYSTAT 2011*, (2011) [[DOI:10.5170/CERN-2011-006.115](#)] [[arXiv:1103.0354](#)] [[INSPIRE](#)].
- [90] CMS collaboration, *The CMS statistical analysis and combination tool: combine*, *Comput. Softw. Big Sci.* **8** (2024) 19 [[arXiv:2404.06614](#)] [[INSPIRE](#)].
- [91] W. Verkerke and D.P. Kirkby, *The RooFit toolkit for data modeling*, *eConf C* **0303241** (2003) MOLT007 [[physics/0306116](#)] [[INSPIRE](#)].
- [92] L. Moneta et al., *The RooStats project*, *PoS ACAT2010* (2010) 057 [[arXiv:1009.1003](#)] [[INSPIRE](#)].
- [93] CMS collaboration, *Object definitions for top quark analyses at the particle level*, CMS-NOTE-2017-004, CERN, Geneva, Switzerland (2017).
- [94] M. Cacciari, G.P. Salam and G. Soyez, *The catchment area of jets*, *JHEP* **04** (2008) 005 [[arXiv:0802.1188](#)] [[INSPIRE](#)].
- [95] G. Cowan, *Statistical data analysis*, Clarendon Press, Oxford, U.K. (1998).
- [96] S. Schmitt, *TUnfold: an algorithm for correcting migration effects in high energy physics*, 2012 *JINST* **7** T10003 [[arXiv:1205.6201](#)] [[INSPIRE](#)].
- [97] G. Cowan, K. Cranmer, E. Gross and O. Vitells, *Asymptotic formulae for likelihood-based tests of new physics*, *Eur. Phys. J. C* **71** (2011) 1554 [Erratum *ibid.* **73** (2013) 2501] [[arXiv:1007.1727](#)] [[INSPIRE](#)].
- [98] W.S. Cleveland, *Robust locally weighted regression and smoothing scatterplots*, *J. Amer. Statist. Assoc.* **74** (1979) 829.

- [99] CMS collaboration, *Performance of photon reconstruction and identification with the CMS detector in proton-proton collisions at $\sqrt{s} = 8$ TeV*, *2015 JINST* **10** P08010 [[arXiv:1502.02702](#)] [[INSPIRE](#)].
- [100] CMS collaboration, *Description and performance of track and primary-vertex reconstruction with the CMS tracker*, *2014 JINST* **9** P10009 [[arXiv:1405.6569](#)] [[INSPIRE](#)].
- [101] CMS collaboration, *Measurements of inclusive W and Z cross sections in pp collisions at $\sqrt{s} = 7$ TeV*, *JHEP* **01** (2011) 080 [[arXiv:1012.2466](#)] [[INSPIRE](#)].
- [102] CMS collaboration, *Measurement of the inelastic proton-proton cross section at $\sqrt{s} = 13$ TeV*, *JHEP* **07** (2018) 161 [[arXiv:1802.02613](#)] [[INSPIRE](#)].
- [103] CMS collaboration, *Luminosity measurement in proton-proton collisions at 13.6 TeV in 2022 at CMS*, CMS-PAS-LUM-22-001, CERN, Geneva, Switzerland (2024).
- [104] CMS collaboration, *Precision luminosity measurement in proton-proton collisions at $\sqrt{s} = 13$ TeV in 2015 and 2016 at CMS*, *Eur. Phys. J. C* **81** (2021) 800 [[arXiv:2104.01927](#)] [[INSPIRE](#)].
- [105] P. Skands, S. Carrazza and J. Rojo, *Tuning PYTHIA 8.1: the Monash 2013 tune*, *Eur. Phys. J. C* **74** (2014) 3024 [[arXiv:1404.5630](#)] [[INSPIRE](#)].
- [106] S. Argyropoulos and T. Sjöstrand, *Effects of color reconnection on $t\bar{t}$ final states at the LHC*, *JHEP* **11** (2014) 043 [[arXiv:1407.6653](#)] [[INSPIRE](#)].
- [107] CMS collaboration, *CMS Pythia 8 colour reconnection tunes based on underlying-event data*, *Eur. Phys. J. C* **83** (2023) 587 [[arXiv:2205.02905](#)] [[INSPIRE](#)].
- [108] CMS collaboration, *Investigations of the impact of the parton shower tuning in Pythia 8 in the modelling of $t\bar{t}$ at $\sqrt{s} = 8$ and 13 TeV*, CMS-PAS-TOP-16-021, CERN, Geneva, Switzerland (2016).
- [109] ATLAS and CMS collaborations, *Combination of measurements of the top quark mass from data collected by the ATLAS and CMS experiments at $\sqrt{s} = 7$ and 8 TeV*, *Phys. Rev. Lett.* **132** (2024) 261902 [[arXiv:2402.08713](#)] [[INSPIRE](#)].
- [110] CMS collaboration, *Measurement of differential cross sections for top quark pair production using the lepton+jets final state in proton-proton collisions at 13 TeV*, *Phys. Rev. D* **95** (2017) 092001 [[arXiv:1610.04191](#)] [[INSPIRE](#)].
- [111] CMS collaboration, *Measurement of the differential cross section for top quark pair production in pp collisions at $\sqrt{s} = 8$ TeV*, *Eur. Phys. J. C* **75** (2015) 542 [[arXiv:1505.04480](#)] [[INSPIRE](#)].
- [112] CMS collaboration, *Measurement of the $t\bar{t}$ production cross section in the all-jets final state in pp collisions at $\sqrt{s} = 8$ TeV*, *Eur. Phys. J. C* **76** (2016) 128 [[arXiv:1509.06076](#)] [[INSPIRE](#)].
- [113] M. Czakon et al., *Top-pair production at the LHC through NNLO QCD and NLO EW*, *JHEP* **10** (2017) 186 [[arXiv:1705.04105](#)] [[INSPIRE](#)].
- [114] CMS collaboration, *Determination of jet energy calibration and transverse momentum resolution in CMS*, *2011 JINST* **6** P11002 [[arXiv:1107.4277](#)] [[INSPIRE](#)].
- [115] CMS collaboration, *Measurement of the top quark polarization and $t\bar{t}$ spin correlations using dilepton final states in proton-proton collisions at $\sqrt{s} = 13$ TeV*, *Phys. Rev. D* **100** (2019) 072002 [[arXiv:1907.03729](#)] [[INSPIRE](#)].

The CMS collaboration

Yerevan Physics Institute, Yerevan, Armenia

A. Hayrapetyan, A. Tumasyan¹

Institut für Hochenergiephysik, Vienna, Austria

W. Adam¹, J.W. Andrejkovic, T. Bergauer¹, S. Chatterjee¹, K. Damanakis¹, M. Dragicevic¹, P.S. Hussain¹, M. Jeitler^{1,2}, N. Krammer¹, A. Li¹, D. Liko¹, I. Mikulec¹, J. Schieck^{1,2}, R. Schöfbeck¹, D. Schwarz¹, M. Sonawane¹, W. Waltenberger¹, C.-E. Wulz^{1,2}

Universiteit Antwerpen, Antwerpen, Belgium

T. Janssen¹, T. Van Laer, P. Van Mechelen¹

Vrije Universiteit Brussel, Brussel, Belgium

N. Breugelmans, J. D'Hondt¹, S. Dansana¹, A. De Moor¹, M. Delcourt¹, F. Heyen, S. Lowette¹, I. Makarenko¹, D. Müller¹, S. Tavernier¹, M. Tytgat^{1,3}, G.P. Van Onsem¹, S. Van Putte¹, D. Vannerom¹

Université Libre de Bruxelles, Bruxelles, Belgium

B. Bilin¹, B. Clerbaux¹, A.K. Das, G. De Lentdecker¹, H. Evard¹, L. Favart¹, P. Gianneios¹, J. Jaramillo¹, A. Khalilzadeh, F.A. Khan¹, K. Lee¹, M. Mahdavikhorrami¹, A. Malara¹, S. Paredes¹, M.A. Shahzad, L. Thomas¹, M. Vanden Bemden¹, C. Vander Velde¹, P. Vanlaer¹

Ghent University, Ghent, Belgium

M. De Coen¹, D. Dobur¹, G. Gokbulut¹, Y. Hong¹, J. Knolle¹, L. Lambrecht¹, D. Marckx¹, K. Mota Amarilo¹, K. Skovpen¹, N. Van Den Bossche¹, J. van der Linden¹, L. Wezenbeek¹

Université Catholique de Louvain, Louvain-la-Neuve, Belgium

A. Benecke¹, A. Bethani¹, G. Bruno¹, C. Caputo¹, J. De Favereau De Jeneret¹, C. Delaere¹, I.S. Donertas¹, A. Giannanco¹, A.O. Guzel¹, Sa. Jain¹, V. Lemaitre, J. Lidrych¹, P. Mastrapasqua¹, T.T. Tran¹, S. Wertz¹

Centro Brasileiro de Pesquisas Fisicas, Rio de Janeiro, Brazil

G.A. Alves¹, M. Alves Gallo Pereira¹, E. Coelho¹, G. Correia Silva¹, C. Hensel¹, T. Menezes De Oliveira¹, C. Mora Herrera^{1,4}, A. Moraes¹, P. Rebello Teles¹, M. Soeiro, A. Vilela Pereira^{1,4}

Universidade do Estado do Rio de Janeiro, Rio de Janeiro, Brazil

W.L. Aldá Júnior¹, M. Barroso Ferreira Filho¹, H. Brandao Malbouisson¹, W. Carvalho¹, J. Chinellato⁵, E.M. Da Costa¹, G.G. Da Silveira^{1,6}, D. De Jesus Damiao¹, S. Fonseca De Souza¹, R. Gomes De Souza, T. Laux Kuhn, M. Macedo¹, J. Martins^{1,7}, L. Mundim¹, H. Nogima¹, J.P. Pinheiro¹, A. Santoro¹, A. Sznajder¹, M. Thiel¹

Universidade Estadual Paulista, Universidade Federal do ABC, São Paulo, Brazil

C.A. Bernardes^{1,6}, L. Calligaris¹, T.R. Fernandez Perez Tomei¹, E.M. Gregores¹, I. Maietto Silverio¹, P.G. Mercadante¹, S.F. Novaes¹, B. Orzari¹, Sandra S. Padula¹

Institute for Nuclear Research and Nuclear Energy, Bulgarian Academy of Sciences, Sofia, Bulgaria

A. Aleksandrov , G. Antchev , R. Hadjiiska , P. Iaydjiev , M. Misheva , M. Shopova , G. Sultanov

University of Sofia, Sofia, Bulgaria

A. Dimitrov , L. Litov , B. Pavlov , P. Petkov , A. Petrov , E. Shumka

Instituto De Alta Investigación, Universidad de Tarapacá, Casilla 7 D, Arica, Chile

S. Keshri , D. Laroze , S. Thakur

Beihang University, Beijing, China

T. Cheng , T. Javaid , L. Yuan

Department of Physics, Tsinghua University, Beijing, China

Z. Hu , Z. Liang, J. Liu

Institute of High Energy Physics, Beijing, China

G.M. Chen ⁸, H.S. Chen ⁸, M. Chen ⁸, F. Iemmi , C.H. Jiang, A. Kapoor ⁹, H. Liao , Z.-A. Liu ¹⁰, R. Sharma ¹¹, J.N. Song¹⁰, J. Tao , C. Wang⁸, J. Wang , Z. Wang⁸, H. Zhang , J. Zhao

State Key Laboratory of Nuclear Physics and Technology, Peking University, Beijing, China

A. Agapitos , Y. Ban , S. Deng , B. Guo, C. Jiang , A. Levin , C. Li , Q. Li , Y. Mao, S. Qian, S.J. Qian , X. Qin, X. Sun , D. Wang , H. Yang, L. Zhang , Y. Zhao, C. Zhou

Guangdong Provincial Key Laboratory of Nuclear Science and Guangdong-Hong Kong Joint Laboratory of Quantum Matter, South China Normal University, Guangzhou, China

S. Yang

Sun Yat-Sen University, Guangzhou, China

Z. You

University of Science and Technology of China, Hefei, China

K. Jaffel , N. Lu

Nanjing Normal University, Nanjing, China

G. Bauer¹², B. Li, K. Yi ^{13,14}, J. Zhang

Institute of Modern Physics and Key Laboratory of Nuclear Physics and Ion-beam Application (MOE) — Fudan University, Shanghai, China

X. Gao ¹⁵, Y. Li

Zhejiang University, Hangzhou, Zhejiang, ChinaZ. Lin¹⁰, C. Lu¹⁰, M. Xiao¹⁰**Universidad de Los Andes, Bogota, Colombia**C. Avila¹¹, D.A. Barbosa Trujillo, A. Cabrera¹¹, C. Florez¹¹, J. Fraga¹¹, J.A. Reyes Vega**Universidad de Antioquia, Medellin, Colombia**F. Ramirez¹², C. Rendón, M. Rodriguez¹², A.A. Ruales Barbosa¹², J.D. Ruiz Alvarez¹²**University of Split, Faculty of Electrical Engineering, Mechanical Engineering and Naval Architecture, Split, Croatia**D. Giljanovic¹³, N. Godinovic¹³, D. Lelas¹³, A. Sculac¹³**University of Split, Faculty of Science, Split, Croatia**M. Kovac¹⁴, A. Petkovic, T. Sculac¹⁴**Institute Rudjer Boskovic, Zagreb, Croatia**P. Bargassa¹⁵, V. Brigljevic¹⁵, B.K. Chitroda¹⁵, D. Ferencek¹⁵, K. Jakovcic, A. Starodumov¹⁶, T. Susa¹⁵**University of Cyprus, Nicosia, Cyprus**A. Attikis¹⁷, K. Christoforou¹⁷, A. Hadjigapiou, C. Leonidou¹⁷, J. Mousa¹⁷, C. Nicolaou, L. Paizanos, F. Ptochos¹⁷, P.A. Razis¹⁷, H. Rykaczewski, H. Saka¹⁷, A. Stepennov¹⁷**Charles University, Prague, Czech Republic**M. Finger¹⁸, M. Finger Jr.¹⁸, A. Kveton¹⁸**Universidad San Francisco de Quito, Quito, Ecuador**E. Carrera Jarrin¹⁹**Academy of Scientific Research and Technology of the Arab Republic of Egypt, Egyptian Network of High Energy Physics, Cairo, Egypt**H. Abdalla²⁰¹⁷, S. Abu Zeid²⁰¹⁸, Y. Assran^{19,20}**Center for High Energy Physics (CHEP-FU), Fayoum University, El-Fayoum, Egypt**M. Abdullah Al-Mashad²¹, M.A. Mahmoud²¹**National Institute of Chemical Physics and Biophysics, Tallinn, Estonia**K. Ehataht²², M. Kadastik, T. Lange²², S. Nandan²², C. Nielsen²², J. Pata²², M. Raidal²², L. Tani²², C. Veelken²²**Department of Physics, University of Helsinki, Helsinki, Finland**H. Kirschenmann²³, K. Osterberg²³, M. Voutilainen²³

Helsinki Institute of Physics, Helsinki, Finland

S. Barthuar , N. Bin Norjoharuddeen , E. Brücken , F. Garcia , P. Inkaew ,
 K.T.S. Kallonen , T. Lampén , K. Lassila-Perini , S. Lehti , T. Lindén , M. Myllymäki ,
 M.m. Rantanen , H. Siikonen , J. Tuominiemi 

Lappeenranta-Lahti University of Technology, Lappeenranta, Finland

P. Luukka , H. Petrow 

IRFU, CEA, Université Paris-Saclay, Gif-sur-Yvette, France

M. Besancon , F. Couderc , M. Dejardin , D. Denegri, J.L. Faure, F. Ferri , S. Ganjour ,
 P. Gras , G. Hamel de Monchenault , M. Kumar , V. Lohezic , J. Malcles , F. Orlandi ,
 L. Portales , A. Rosowsky , M.Ö. Sahin , A. Savoy-Navarro ²¹, P. Simkina , M. Titov ,
 M. Tornago 

Laboratoire Leprince-Ringuet, CNRS/IN2P3, Ecole Polytechnique, Institut Polytechnique de Paris, Palaiseau, France

F. Beaudette , G. Boldrini , P. Busson , A. Cappati , C. Charlot , M. Chiusi , F. Damas ,
 O. Davignon , A. De Wit , I.T. Ehle , B.A. Fontana Santos Alves , S. Ghosh , A. Gilbert ,
 R. Granier de Cassagnac , A. Hakimi , B. Harikrishnan , L. Kalipoliti , G. Liu , M. Nguyen ,
 C. Ochando , R. Salerno , J.B. Sauvan , Y. Sirois , L. Urda Gómez , E. Vernazza ,
 A. Zabi , A. Zghiche 

Université de Strasbourg, CNRS, IPHC UMR 7178, Strasbourg, France

J.-L. Agram ²², J. Andrea , D. Apparu , D. Bloch , J.-M. Brom , E.C. Chabert ,
 C. Collard , S. Falke , U. Goerlach , R. Haeberle , A.-C. Le Bihan , M. Meena , O. Poncet ,
 G. Saha , M.A. Sessini , P. Van Hove , P. Vaucelle 

Centre de Calcul de l’Institut National de Physique Nucléaire et de Physique des Particules, CNRS/IN2P3, Villeurbanne, France

A. Di Florio 

Institut de Physique des 2 Infinis de Lyon (IP2I), Villeurbanne, France

D. Amram, S. Beauceron , B. Blançon , G. Boudoul , N. Chanon , D. Contardo ,
 P. Depasse , C. Dozen ²³, H. El Mamouni, J. Fay , S. Gascon , M. Gouzevitch , C. Greenberg,
 G. Grenier , B. Ille , E. Jourd’huy, I.B. Laktineh, M. Lethuillier , L. Mirabito, S. Perries,
 A. Purohit , M. Vander Donckt , P. Verdier , J. Xiao 

Georgian Technical University, Tbilisi, Georgia

I. Lomidze , T. Toriashvili ²⁴, Z. Tsamalaidze ¹⁶

RWTH Aachen University, I. Physikalisches Institut, Aachen, Germany

V. Botta , S. Consuegra Rodríguez , L. Feld , K. Klein , M. Lipinski , D. Meuser ,
 A. Pauls , D. Pérez Adán , N. Röwert , M. Teroerde 

RWTH Aachen University, III. Physikalisches Institut A, Aachen, Germany

S. Diekmann , A. Dodonova , N. Eich , D. Eliseev , F. Engelke , J. Erdmann ,
 M. Erdmann , P. Fackeldey , B. Fischer , T. Hebbeker , K. Hoepfner , F. Ivone , A. Jung ,

M.y. Lee^{ID}, F. Mausolf^{ID}, M. Merschmeyer^{ID}, A. Meyer^{ID}, S. Mukherjee^{ID}, D. Noll^{ID}, F. Nowotny, A. Pozdnyakov^{ID}, Y. Rath, W. Redjeb^{ID}, F. Rehm, H. Reithler^{ID}, V. Sarkisovi^{ID}, A. Schmidt^{ID}, C. Seth, A. Sharma^{ID}, J.L. Spah^{ID}, A. Stein^{ID}, F. Torres Da Silva De Araujo^{ID}²⁵, S. Wiedenbeck^{ID}, S. Zaleski

RWTH Aachen University, III. Physikalisches Institut B, Aachen, Germany

C. Dziewok^{ID}, G. Flügge^{ID}, T. Kress^{ID}, A. Nowack^{ID}, O. Pooth^{ID}, A. Stahl^{ID}, T. Ziemons^{ID}, A. Zottz^{ID}

Deutsches Elektronen-Synchrotron, Hamburg, Germany

H. Aarup Petersen^{ID}, M. Aldaya Martin^{ID}, J. Alimena^{ID}, S. Amoroso, Y. An^{ID}, J. Bach^{ID}, S. Baxter^{ID}, M. Bayatmakou^{ID}, H. Becerril Gonzalez^{ID}, O. Behnke^{ID}, A. Belvedere^{ID}, F. Blekman^{ID}²⁶, K. Borras^{ID}²⁷, A. Campbell^{ID}, A. Cardini^{ID}, C. Cheng, F. Colombina^{ID}, G. Eckerlin, D. Eckstein^{ID}, L.I. Estevez Banos^{ID}, O. Filatov^{ID}, E. Gallo^{ID}²⁶, A. Geiser^{ID}, V. Guglielmi^{ID}, M. Guthoff^{ID}, A. Hinzmamn^{ID}, L. Jeppe^{ID}, B. Kaech^{ID}, M. Kasemann^{ID}, C. Kleinwort^{ID}, R. Kogler^{ID}, M. Komm^{ID}, D. Krücker^{ID}, W. Lange, D. Leyva Pernia^{ID}, K. Lipka^{ID}²⁸, W. Lohmann^{ID}²⁹, F. Lorkowski^{ID}, R. Mankel^{ID}, I.-A. Melzer-Pellmann^{ID}, M. Mendizabal Morentin^{ID}, A.B. Meyer^{ID}, G. Milella^{ID}, K. Moral Figueroa^{ID}, A. Mussgiller^{ID}, L.P. Nair^{ID}, J. Niedziela^{ID}, A. Nürnberg^{ID}, Y. Otariid, J. Park^{ID}, E. Ranken^{ID}, A. Raspereza^{ID}, D. Rastorguev^{ID}, J. Rübenach, L. Rygaard, A. Saggio^{ID}, M. Scham^{ID}^{30,27}, S. Schnake^{ID}²⁷, P. Schütze^{ID}, C. Schwanenberger^{ID}²⁶, D. Selivanova^{ID}, K. Sharko^{ID}, M. Shchedrolosiev^{ID}, D. Stafford, F. Vazzoler^{ID}, A. Ventura Barroso^{ID}, R. Walsh^{ID}, D. Wang^{ID}, Q. Wang^{ID}, Y. Wen^{ID}, K. Wichmann, L. Wiens^{ID}²⁷, C. Wissing^{ID}, Y. Yang^{ID}, A. Zimermann Castro Santos^{ID}

University of Hamburg, Hamburg, Germany

A. Albrecht^{ID}, S. Albrecht^{ID}, M. Antonello^{ID}, S. Bein^{ID}, L. Benato^{ID}, S. Bollweg, M. Bonanomi^{ID}, P. Connor^{ID}, K. El Morabit^{ID}, Y. Fischer^{ID}, E. Garutti^{ID}, A. Grohsjean^{ID}, J. Haller^{ID}, H.R. Jabusch^{ID}, G. Kasieczka^{ID}, P. Keicher, R. Klanner^{ID}, W. Korcari^{ID}, T. Kramer^{ID}, C.c. Kuo, V. Kutzner^{ID}, F. Labe^{ID}, J. Lange^{ID}, A. Lobanov^{ID}, C. Matthies^{ID}, L. Moureaux^{ID}, M. Mrowietz, A. Nigamova^{ID}, Y. Nissan, A. Paasch^{ID}, K.J. Pena Rodriguez^{ID}, T. Quadfasel^{ID}, B. Raciti^{ID}, M. Rieger^{ID}, D. Savoiu^{ID}, J. Schindler^{ID}, P. Schleper^{ID}, M. Schröder^{ID}, J. Schwandt^{ID}, M. Sommerhalder^{ID}, H. Stadie^{ID}, G. Steinbrück^{ID}, A. Tews, M. Wolf^{ID}

Karlsruher Institut fuer Technologie, Karlsruhe, Germany

S. Brommer^{ID}, M. Burkart, E. Butz^{ID}, T. Chwalek^{ID}, A. Dierlamm^{ID}, A. Droll, U. Elicabuk, N. Faltermann^{ID}, M. Giffels^{ID}, A. Gottmann^{ID}, F. Hartmann^{ID}³¹, R. Hofsaess^{ID}, M. Horzela^{ID}, U. Husemann^{ID}, J. Kieseler^{ID}, M. Klute^{ID}, R. Koppenhöfer^{ID}, J.M. Lawhorn^{ID}, M. Link, A. Lintuluoto^{ID}, S. Maier^{ID}, S. Mitra^{ID}, M. Mormile^{ID}, Th. Müller^{ID}, M. Neukum, M. Oh^{ID}, E. Pfeffer^{ID}, M. Presilla^{ID}, G. Quast^{ID}, K. Rabbertz^{ID}, B. Regnery^{ID}, N. Shadskiy^{ID}, I. Shvetsov^{ID}, H.J. Simonis^{ID}, L. Sowa, L. Stockmeier, K. Tauqueer, M. Toms^{ID}, N. Trevisani^{ID}, R.F. Von Cube^{ID}, M. Wassmer^{ID}, S. Wieland^{ID}, F. Wittig, R. Wolf^{ID}, X. Zuo^{ID}

Institute of Nuclear and Particle Physics (INPP), NCSR Demokritos, Aghia Paraskevi, Greece

G. Anagnostou, G. Daskalakis^{ID}, A. Kyriakis, A. Papadopoulos³¹, A. Stakia^{ID}

National and Kapodistrian University of Athens, Athens, Greece

P. Kontaxakis , G. Melachroinos, Z. Painesis , I. Papavergou , I. Paraskevas , N. Saoulidou , K. Theofilatos , E. Tziaferi , K. Vellidis , I. Zisopoulos

National Technical University of Athens, Athens, Greece

G. Bakas , T. Chatzistavrou, G. Karapostoli , K. Kousouris , I. Papakrivopoulos , E. Siamarkou, G. Tsipolitis , A. Zacharopoulou

University of Ioánnina, Ioánnina, Greece

K. Adamidis, I. Bestintzanos, I. Evangelou , C. Foudas, C. Kamtsikis, P. Katsoulis, P. Kokkas , P.G. Kosmoglou Kiouseoglou , N. Manthos , I. Papadopoulos , J. Strologas

HUN-REN Wigner Research Centre for Physics, Budapest, Hungary

C. Hajdu , D. Horvath ^{32,33}, K. Márton, A.J. Rádl ³⁴, F. Sikler , V. Veszpremi 

MTA-ELTE Lendület CMS Particle and Nuclear Physics Group, Eötvös Loránd University, Budapest, Hungary

M. Csand , K. Farkas , A. Fehrkuti ³⁵, M.M.A. Gadallah ³⁶, . Kadlecik , P. Major , G. Pasztor , G.I. Veres 

Faculty of Informatics, University of Debrecen, Debrecen, Hungary

L. Olah , B. Ujvari 

Institute of Nuclear Research ATOMKI, Debrecen, Hungary

G. Bencze, S. Czellar, J. Molnar, Z. Szillasi

Karoly Robert Campus, MATE Institute of Technology, Gyongyos, Hungary

F. Nemes , T. Novak 

Panjab University, Chandigarh, India

S. Bansal , S.B. Beri, V. Bhatnagar , G. Chaudhary , S. Chauhan , N. Dhingra  ³⁷, A. Kaur , A. Kaur , H. Kaur , M. Kaur , S. Kumar , T. Sheokand, J.B. Singh , A. Singla

University of Delhi, Delhi, India

A. Ahmed , A. Bhardwaj , A. Chhetri , B.C. Choudhary , A. Kumar , A. Kumar , M. Naimuddin , K. Ranjan , M.K. Saini, S. Saumya

Saha Institute of Nuclear Physics, HBNI, Kolkata, India

S. Baradia , S. Barman  ³⁸, S. Bhattacharya , S. Das Gupta, S. Dutta , S. Dutta, S. Sarkar

Indian Institute of Technology Madras, Madras, India

M.M. Ameen , P.K. Behera , S.C. Behera , S. Chatterjee , G. Dash , P. Jana , P. Kalbhor , S. Kamble , J.R. Komaragiri ³⁹, D. Kumar ³⁹, T. Mishra , B. Parida , P.R. Pujahari , N.R. Saha , A. Sharma , A.K. Sikdar , R.K. Singh, P. Verma, S. Verma , A. Vijay

Tata Institute of Fundamental Research-A, Mumbai, India

S. Dugad, G.B. Mohanty , M. Shelake, P. Suryadevara

Tata Institute of Fundamental Research-B, Mumbai, India

A. Bala , S. Banerjee , R.M. Chatterjee, M. Guchait , Sh. Jain , A. Jaiswal, S. Kumar ,
G. Majumder , K. Mazumdar , S. Parolia , A. Thachayath 

National Institute of Science Education and Research, An OCC of Homi Bhabha National Institute, Bhubaneswar, Odisha, India

S. Bahinipati ⁴⁰, C. Kar , D. Maity ⁴¹, P. Mal , V.K. Muraleedharan Nair Bindhu ⁴¹,
K. Naskar ⁴¹, A. Nayak ⁴¹, S. Nayak, K. Pal, P. Sadangi, S.K. Swain , S. Varghese ⁴¹,
D. Vats ⁴¹

Indian Institute of Science Education and Research (IISER), Pune, India

S. Acharya ⁴², A. Alpana , S. Dube , B. Gomber ⁴², P. Hazarika , B. Kansal , A. Laha ,
B. Sahu ⁴², S. Sharma , K.Y. Vaish 

Isfahan University of Technology, Isfahan, Iran

H. Bakhshiansohi ⁴³, A. Jafari , M. Zeinali ⁴⁵

Institute for Research in Fundamental Sciences (IPM), Tehran, Iran

S. Bashiri, S. Chenarani ⁴⁶, S.M. Etesami , Y. Hosseini , M. Khakzad , E. Khazaie ,
M. Mohammadi Najafabadi , S. Tizchang ⁴⁷

University College Dublin, Dublin, Ireland

M. Felcini , M. Grunewald 

INFN Sezione di Bari^a, Università di Bari^b, Politecnico di Bari^c, Bari, Italy

M. Abbrescia , A. Colaleo , D. Creanza , B. D'Anzi , N. De Filippis ,
M. De Palma , W. Elmetenawee ,⁴⁸ L. Fiore , G. Iaselli , L. Longo , M. Louka ,
G. Maggi , M. Maggi , I. Margjeka , V. Mastrapasqua , S. My , S. Nuzzo ,
A. Pellecchia , A. Pompili , G. Pugliese , R. Radogna , D. Ramos , A. Ranieri ,
L. Silvestris , F.M. Simone , Ü. Sözbilir , A. Stamerra , D. Troiano , R. Venditti ,
P. Verwilligen , A. Zaza ^{a,b}

INFN Sezione di Bologna^a, Università di Bologna^b, Bologna, Italy

G. Abbiendi , C. Battilana , D. Bonacorsi , P. Capiluppi , A. Castro †,^{a,b},
F.R. Cavallo , M. Cuffiani , G.M. Dallavalle , T. Diotalevi , F. Fabbri ,
A. Fanfani , D. Fasanella , P. Giacomelli , L. Giommi , C. Grandi , L. Guiducci ,
S. Lo Meo , M. Lorusso , L. Lunerti , S. Marcellini , G. Masetti , F.L. Navarria ,
G. Paggi , A. Perrotta , F. Primavera , A.M. Rossi , S. Rossi Tisbeni ,
T. Rovelli , G.P. Siroli ^{a,b}

INFN Sezione di Catania^a, Università di Catania^b, Catania, Italy

S. Costa , A. Di Mattia , A. Lapertosa , R. Potenza^{a,b}, A. Tricomi ,^{a,b,50}, C. Tuve 

INFN Sezione di Firenze^a, Università di Firenze^b, Firenze, Italy

P. Assiouras , G. Barbagli , G. Bardelli , B. Camaiana , A. Cassese , R. Ceccarelli ,
V. Ciulli , C. Civinini , R. D'Alessandro , E. Focardi , T. Kello^a, G. Latino ,

P. Lenzi $\text{ID}^{a,b}$, M. Lizzo ID^a , M. Meschini ID^a , S. Paoletti ID^a , A. Papanastassiou a,b , G. Sguazzoni ID^a , L. Viliani ID^a

INFN Laboratori Nazionali di Frascati, Frascati, Italy

L. Benussi ID , S. Bianco ID , S. Meola ID^{51} , D. Piccolo ID

INFN Sezione di Genova^a, Università di Genova^b, Genova, Italy

P. Chatagnon ID^a , F. Ferro ID^a , E. Robutti ID^a , S. Tosi $\text{ID}^{a,b}$

INFN Sezione di Milano-Bicocca^a, Università di Milano-Bicocca^b, Milano, Italy

A. Benaglia ID^a , F. Brivio ID^a , F. Cetorelli $\text{ID}^{a,b}$, F. De Guio $\text{ID}^{a,b}$, M.E. Dinardo $\text{ID}^{a,b}$, P. Dini ID^a , S. Gennai ID^a , R. Gerosa $\text{ID}^{a,b}$, A. Ghezzi $\text{ID}^{a,b}$, P. Govoni $\text{ID}^{a,b}$, L. Guzzi ID^a , M.T. Lucchini $\text{ID}^{a,b}$, M. Malberti ID^a , S. Malvezzi ID^a , A. Massironi ID^a , D. Menasce ID^a , L. Moroni ID^a , M. Paganoni $\text{ID}^{a,b}$, S. Palluotto $\text{ID}^{a,b}$, D. Pedrini ID^a , A. Perego $\text{ID}^{a,b}$, B.S. Pinolini a , G. Pizzati a,b , S. Ragazzi $\text{ID}^{a,b}$, T. Tabarelli de Fatis $\text{ID}^{a,b}$

INFN Sezione di Napoli^a, Università di Napoli ‘Federico II’^b, Napoli, Italy; Università della Basilicata^c, Potenza, Italy; Scuola Superiore Meridionale (SSM)^d, Napoli, Italy

S. Buontempo ID^a , A. Cagnotta $\text{ID}^{a,b}$, F. Carnevali a,b , N. Cavallo $\text{ID}^{a,c}$, F. Fabozzi $\text{ID}^{a,c}$, A.O.M. Iorio $\text{ID}^{a,b}$, L. Lista $\text{ID}^{a,b,52}$, P. Paolucci $\text{ID}^{a,31}$, B. Rossi ID^a

INFN Sezione di Padova^a, Università di Padova^b, Padova, Italy; Università di Trento^c, Trento, Italy

R. Ardino ID^a , P. Azzi ID^a , N. Bacchetta $\text{ID}^{a,53}$, P. Bortignon ID^a , G. Bortolato a,b , A. Bragagnolo $\text{ID}^{a,b}$, A.C.M. Bulla ID^a , R. Carlin $\text{ID}^{a,b}$, P. Checchia ID^a , T. Dorigo ID^a , F. Gasparini $\text{ID}^{a,b}$, U. Gasparini $\text{ID}^{a,b}$, S. Giorgetti a , E. Lusiani ID^a , M. Margoni $\text{ID}^{a,b}$, A.T. Meneguzzo $\text{ID}^{a,b}$, M. Michelotto ID^a , M. Migliorini $\text{ID}^{a,b}$, J. Pazzini $\text{ID}^{a,b}$, P. Ronchese $\text{ID}^{a,b}$, R. Rossin $\text{ID}^{a,b}$, F. Simonetto $\text{ID}^{a,b}$, M. Tosi $\text{ID}^{a,b}$, A. Triossi $\text{ID}^{a,b}$, S. Ventura ID^a , M. Zanetti $\text{ID}^{a,b}$, P. Zotto $\text{ID}^{a,b}$, A. Zucchetta $\text{ID}^{a,b}$, G. Zumerle $\text{ID}^{a,b}$

INFN Sezione di Pavia^a, Università di Pavia^b, Pavia, Italy

A. Braghieri ID^a , S. Calzaferri ID^a , D. Fiorina ID^a , P. Montagna $\text{ID}^{a,b}$, V. Re ID^a , C. Riccardi $\text{ID}^{a,b}$, P. Salvini ID^a , I. Vai $\text{ID}^{a,b}$, P. Vitulo $\text{ID}^{a,b}$

INFN Sezione di Perugia^a, Università di Perugia^b, Perugia, Italy

S. Ajmal $\text{ID}^{a,b}$, M.E. Ascoli a,b , G.M. Bilei ID^a , C. Carrivale a,b , D. Ciangottini $\text{ID}^{a,b}$, L. Fanò $\text{ID}^{a,b}$, M. Magherini $\text{ID}^{a,b}$, V. Mariani $\text{ID}^{a,b}$, M. Menichelli ID^a , F. Moscatelli $\text{ID}^{a,54}$, A. Rossi $\text{ID}^{a,b}$, A. Santocchia $\text{ID}^{a,b}$, D. Spiga ID^a , T. Tedeschi $\text{ID}^{a,b}$

INFN Sezione di Pisa^a, Università di Pisa^b, Scuola Normale Superiore di Pisa^c, Pisa, Italy; Università di Siena^d, Siena, Italy

C. Aimè ID^a , C.A. Alexe $\text{ID}^{a,c}$, P. Asenov $\text{ID}^{a,b}$, P. Azzurri ID^a , G. Bagliesi ID^a , R. Bhattacharya ID^a , L. Bianchini $\text{ID}^{a,b}$, T. Boccali ID^a , E. Bossini ID^a , D. Bruschini $\text{ID}^{a,c}$, R. Castaldi ID^a , M.A. Ciocci $\text{ID}^{a,b}$, M. Cipriani $\text{ID}^{a,b}$, V. D’Amante $\text{ID}^{a,d}$, R. Dell’Orso ID^a , S. Donato ID^a , A. Giassi ID^a , F. Ligabue $\text{ID}^{a,c}$, A.C. Marini ID^a , D. Matos Figueiredo ID^a , A. Messineo $\text{ID}^{a,b}$, S. Mishra ID^a , M. Musich $\text{ID}^{a,b}$, F. Palla ID^a ,

A. Rizzi ^{a,b}, G. Rolandi ^{a,c}, S. Roy Chowdhury ^a, T. Sarkar ^a, A. Scribano ^a, P. Spagnolo ^a, R. Tenchini ^a, G. Tonelli ^{a,b}, N. Turini ^{a,d}, F. Vaselli ^{a,c}, A. Venturi ^a, P.G. Verdini ^a

INFN Sezione di Roma^a, Sapienza Università di Roma^b, Roma, Italy

C. Baldenegro Barrera ^{a,b}, P. Barria ^a, C. Basile ^{a,b}, F. Cavallari ^a, L. Cunqueiro Mendez ^{a,b}, D. Del Re ^{a,b}, E. Di Marco ^{a,b}, M. Diemoz ^a, F. Errico ^{a,b}, E. Longo ^{a,b}, L. Martikainen ^{a,b}, J. Mijuskovic ^{a,b}, G. Organtini ^{a,b}, F. Pandolfi ^a, R. Paramatti ^{a,b}, C. Quaranta ^{a,b}, S. Rahatlou ^{a,b}, C. Rovelli ^a, F. Santanastasio ^{a,b}, L. Soffi ^a

INFN Sezione di Torino^a, Università di Torino^b, Torino, Italy; Università del Piemonte Orientale^c, Novara, Italy

N. Amapane ^{a,b}, R. Arcidiacono ^{a,c}, S. Argiro ^{a,b}, M. Arneodo ^{a,c}, N. Bartosik ^a, R. Bellan ^{a,b}, A. Bellora ^{a,b}, C. Biino ^a, C. Borca ^{a,b}, N. Cartiglia ^a, M. Costa ^{a,b}, R. Covarelli ^{a,b}, N. Demaria ^a, L. Finco ^a, M. Grippo ^{a,b}, B. Kiani ^{a,b}, F. Legger ^a, F. Luongo ^{a,b}, C. Mariotti ^a, L. Markovic ^{a,b}, S. Maselli ^a, A. Mecca ^{a,b}, L. Menzio ^{a,b}, P. Meridiani ^a, E. Migliore ^{a,b}, M. Monteno ^a, R. Mulargia ^a, M.M. Obertino ^{a,b}, G. Ortona ^a, L. Pacher ^{a,b}, N. Pastrone ^a, M. Pelliccioni ^a, M. Ruspa ^{a,c}, F. Siviero ^{a,b}, V. Sola ^{a,b}, A. Solano ^{a,b}, A. Staiano ^a, C. Tarricone ^{a,b}, D. Trocino ^a, G. Umoret ^{a,b}, R. White ^{a,b}

INFN Sezione di Trieste^a, Università di Trieste^b, Trieste, Italy

J. Babbar ^{a,b}, S. Belforte ^a, V. Cadelise ^{a,b}, M. Casarsa ^a, F. Cossutti ^a, K. De Leo ^a, G. Della Ricca ^{a,b}

Kyungpook National University, Daegu, Korea

S. Dogra , J. Hong , B. Kim , J. Kim, D. Lee, H. Lee, S.W. Lee , C.S. Moon , Y.D. Oh , M.S. Ryu , S. Sekmen , B. Tae, Y.C. Yang

Department of Mathematics and Physics — GWNU, Gangneung, Korea

M.S. Kim 

Chonnam National University, Institute for Universe and Elementary Particles, Kwangju, Korea

G. Bak , P. Gwak , H. Kim , D.H. Moon 

Hanyang University, Seoul, Korea

E. Asilar , J. Choi , D. Kim , T.J. Kim , J.A. Merlin, Y. Ryou

Korea University, Seoul, Korea

S. Choi , S. Han, B. Hong , K. Lee, K.S. Lee , S. Lee , J. Yoo 

Kyung Hee University, Department of Physics, Seoul, Korea

J. Goh , S. Yang 

Sejong University, Seoul, Korea

H. S. Kim , Y. Kim, S. Lee

Seoul National University, Seoul, Korea

J. Almond, J.H. Bhyun, J. Choi[✉], J. Choi, W. Jun[✉], J. Kim[✉], Y.W. Kim, S. Ko[✉], H. Kwon[✉], H. Lee[✉], J. Lee[✉], J. Lee[✉], B.H. Oh[✉], S.B. Oh[✉], H. Seo[✉], U.K. Yang, I. Yoon[✉]

University of Seoul, Seoul, Korea

W. Jang[✉], D.Y. Kang, Y. Kang[✉], S. Kim[✉], B. Ko, J.S.H. Lee[✉], Y. Lee[✉], I.C. Park[✉], Y. Roh, I.J. Watson[✉]

Yonsei University, Department of Physics, Seoul, Korea

S. Ha[✉], K. Hwang, H.D. Yoo[✉]

Sungkyunkwan University, Suwon, Korea

M. Choi[✉], M.R. Kim[✉], H. Lee, Y. Lee[✉], I. Yu[✉]

College of Engineering and Technology, American University of the Middle East (AUM), Dasman, Kuwait

T. Beyrouty, Y. Gharbia

Kuwait University — College of Science — Department of Physics, Safat, Kuwait

F. Alazemi[✉]

Riga Technical University, Riga, Latvia

K. Dreimanis[✉], A. Gaile[✉], C. Munoz Diaz, D. Osite[✉], G. Pikurs, A. Potrebko[✉], M. Seidel[✉], D. Sidiropoulos Kontos

University of Latvia (LU), Riga, Latvia

N.R. Strautnieks[✉]

Vilnius University, Vilnius, Lithuania

M. Ambrozas[✉], A. Juodagalvis[✉], A. Rinkevicius[✉], G. Tamulaitis[✉]

National Centre for Particle Physics, Universiti Malaya, Kuala Lumpur, Malaysia

I. Yusuff[✉]⁵⁵, Z. Zolkapli

Universidad de Sonora (UNISON), Hermosillo, Mexico

J.F. Benitez[✉], A. Castaneda Hernandez[✉], H.A. Encinas Acosta, L.G. Gallegos Maríñez, M. León Coello[✉], J.A. Murillo Quijada[✉], A. Sehrawat[✉], L. Valencia Palomo[✉]

Centro de Investigacion y de Estudios Avanzados del IPN, Mexico City, Mexico

G. Ayala[✉], H. Castilla-Valdez[✉], H. Crotte Ledesma, E. De La Cruz-Burelo[✉], I. Heredia-De La Cruz[✉]⁵⁶, R. Lopez-Fernandez[✉], J. Mejia Guisao[✉], C.A. Mondragon Herrera, A. Sánchez Hernández[✉]

Universidad Iberoamericana, Mexico City, Mexico

C. Oropeza Barrera[✉], D.L. Ramirez Guadarrama, M. Ramírez García[✉]

Benemerita Universidad Autonoma de Puebla, Puebla, MexicoI. Bautista , I. Pedraza , H.A. Salazar Ibarguen , C. Uribe Estrada **University of Montenegro, Podgorica, Montenegro**I. Bubanja , N. Raicevic **University of Canterbury, Christchurch, New Zealand**P.H. Butler **National Centre for Physics, Quaid-I-Azam University, Islamabad, Pakistan**A. Ahmad , M.I. Asghar, A. Awais , M.I.M. Awan, H.R. Hoorani , W.A. Khan **AGH University of Krakow, Faculty of Computer Science, Electronics and Telecommunications, Krakow, Poland**V. Avati, L. Grzanka , M. Malawski **National Centre for Nuclear Research, Swierk, Poland**H. Bialkowska , M. Bluj , M. Górski , M. Kazana , M. Szleper , P. Zalewski **Institute of Experimental Physics, Faculty of Physics, University of Warsaw, Warsaw, Poland**K. Bunkowski , K. Doroba , A. Kalinowski , M. Konecki , J. Krolikowski , A. Muhammad **Warsaw University of Technology, Warsaw, Poland**K. Pozniak , W. Zabolotny **Laboratório de Instrumentação e Física Experimental de Partículas, Lisboa, Portugal**M. Araujo , D. Bastos , C. Beirão Da Cruz E Silva , A. Boletti , M. Bozzo , T. Camporesi , G. Da Molin , P. Faccioli , M. Gallinaro , J. Hollar , N. Leonardo , G.B. Marozzo, T. Niknejad , A. Petrilli , M. Pisano , J. Seixas , J. Varela , J.W. Wulff**Faculty of Physics, University of Belgrade, Belgrade, Serbia**P. Adzic , P. Milenovic **VINCA Institute of Nuclear Sciences, University of Belgrade, Belgrade, Serbia**D. Devetak, M. Dordevic , J. Milosevic , L. Nadderd , V. Rekovic**Centro de Investigaciones Energéticas Medioambientales y Tecnológicas (CIEMAT), Madrid, Spain**J. Alcaraz Maestre , Cristina F. Bedoya , J.A. Brochero Cifuentes , Oliver M. Carretero , M. Cepeda , M. Cerrada , N. Colino , B. De La Cruz , A. Delgado Peris , A. Escalante Del Valle , D. Fernández Del Val , J.P. Fernández Ramos , J. Flix , M.C. Fouz , O. Gonzalez Lopez , S. Goy Lopez , J.M. Hernandez , M.I. Josa , J. Llorente Merino , E. Martin Viscasillas , D. Moran , C. M. Morcillo Perez , Á. Navarro Tobar , C. Perez Dengra , A. Pérez-Calero Yzquierdo , J. Puerta Pelayo , I. Redondo , S. Sánchez Navas , J. Sastre , J. Vazquez Escobar 

Universidad Autónoma de Madrid, Madrid, SpainJ.F. de Trocóniz **Universidad de Oviedo, Instituto Universitario de Ciencias y Tecnologías Espaciales de Asturias (ICTEA), Oviedo, Spain**

B. Alvarez Gonzalez , J. Cuevas , J. Fernandez Menendez , S. Folgueras ,
 I. Gonzalez Caballero , P. Leguina , E. Palencia Cortezon , J. Prado Pico, C. Ramón Álvarez ,
 V. Rodríguez Bouza , A. Soto Rodríguez , A. Trapote , C. Vico Villalba , P. Vischia 

Instituto de Física de Cantabria (IFCA), CSIC-Universidad de Cantabria, Santander, Spain

S. Bhowmik , S. Blanco Fernández , I.J. Cabrillo , A. Calderon , J. Duarte Campderros ,
 M. Fernandez , G. Gomez , C. Lasosa García , R. Lopez Ruiz , C. Martinez Rivero ,
 P. Martinez Ruiz del Arbol , F. Matorras , P. Matorras Cuevas , E. Navarrete Ramos ,
 J. Piedra Gomez , L. Scodellaro , I. Vila , J.M. Vizan Garcia 

University of Colombo, Colombo, Sri LankaB. Kailasapathy ⁵⁷, D.D.C. Wickramarathna **University of Ruhuna, Department of Physics, Matara, Sri Lanka**W.G.D. Dharmaratna ⁵⁸, K. Liyanage , N. Perera **CERN, European Organization for Nuclear Research, Geneva, Switzerland**

D. Abbaneo , C. Amendola , E. Auffray , G. Auzinger , J. Baechler, D. Barney ,
 A. Bermúdez Martínez , M. Bianco , A.A. Bin Anuar , A. Bocci , L. Borgonovi , C. Botta ,
 E. Brondolin , C. Caillol , G. Cerminara , N. Chernyavskaya , D. d'Enterria , A. Dabrowski ,
 A. David , A. De Roeck , M.M. Defranchis , M. Deile , M. Dobson , G. Franzoni ,
 W. Funk , S. Giani, D. Gigi, K. Gill , F. Glege , J. Hegeman , J.K. Heikkilä , B. Huber,
 V. Innocente , T. James , P. Janot , O. Kaluzinska , O. Karacheban ²⁹, S. Laurila ,
 P. Lecoq , E. Leutgeb , C. Lourenço , L. Malgeri , M. Mannelli , M. Matthewman,
 A. Mehta , F. Meijers , S. Mersi , E. Meschi , V. Milosevic , F. Monti , F. Moortgat ,
 M. Mulders , I. Neutelings , S. Orfanelli, F. Pantaleo , G. Petrucciani , A. Pfeiffer ,
 M. Pierini , H. Qu , D. Rabady , B. Ribeiro Lopes , M. Rovere , H. Sakulin ,
 S. Sanchez Cruz , S. Scarfi , C. Schwick, M. Selvaggi , A. Sharma , K. Shchelina , P. Silva ,
 P. Sphicas ⁵⁹, A.G. Stahl Leiton , A. Steen , S. Summers , D. Treille , P. Tropea ,
 D. Walter , J. Wanczyk , J. Wang, K.A. Wozniak ⁶¹, S. Wuchterl , P. Zehetner , P. Zejdl ,
 W.D. Zeuner

Paul Scherrer Institut, Villigen, Switzerland

T. Bevilacqua ⁶², L. Caminada ⁶², A. Ebrahimi , W. Erdmann , R. Horisberger , Q. Ingram ,
 H.C. Kaestli , D. Kotlinski , C. Lange , M. Missiroli ⁶², L. Noehte ⁶², T. Rohe , A. Samalan

ETH Zurich — Institute for Particle Physics and Astrophysics (IPA), Zurich, Switzerland

T.K. Arrestad , M. Backhaus , G. Bonomelli, A. Calandri , C. Cazzaniga , K. Datta ,
 P. De Bryas Dexmiers D'archiac ⁶⁰, A. De Cosa , G. Dissertori , M. Dittmar, M. Donegà 

F. Eble^{1D}, M. Galli^{1D}, K. Gedia^{1D}, F. Glessgen^{1D}, C. Grab^{1D}, N. Härringer^{1D}, T.G. Harte, D. Hits^{1D}, W. Lustermann^{1D}, A.-M. Lyon^{1D}, R.A. Manzoni^{1D}, M. Marchegiani^{1D}, L. Marchese^{1D}, C. Martin Perez^{1D}, A. Mascellani⁶⁰, F. Nessi-Tedaldi^{1D}, F. Pauss^{1D}, V. Perovic^{1D}, S. Pigazzini^{1D}, B. Ristic^{1D}, F. Riti^{1D}, R. Seidita^{1D}, J. Steggemann⁶⁰, A. Tarabini^{1D}, D. Valsecchi^{1D}, R. Wallny^{1D}

Universität Zürich, Zurich, Switzerland

C. Amsler^{1D}⁶³, P. Bärtschi^{1D}, M.F. Canelli^{1D}, K. Cormier^{1D}, M. Huwiler^{1D}, W. Jin^{1D}, A. Jofrehei^{1D}, B. Kilminster^{1D}, S. Leontsinis^{1D}, S.P. Liechti^{1D}, A. Macchiolo^{1D}, P. Meiring^{1D}, F. Meng^{1D}, U. Molinatti^{1D}, J. Motta^{1D}, A. Reimers^{1D}, P. Robmann, M. Senger^{1D}, E. Shokr, F. Stäger^{1D}, R. Tramontano^{1D}

National Central University, Chung-Li, Taiwan

C. Adloff⁶⁴, D. Bhowmik, C.M. Kuo, W. Lin, P.K. Rout^{1D}, P.C. Tiwari^{1D}³⁹, S.S. Yu^{1D}

National Taiwan University (NTU), Taipei, Taiwan

L. Ceard, K.F. Chen^{1D}, P.s. Chen, Z.g. Chen, A. De Iorio^{1D}, W.-S. Hou^{1D}, T.h. Hsu, Y.w. Kao, S. Karmakar^{1D}, G. Kole^{1D}, Y.y. Li^{1D}, R.-S. Lu^{1D}, E. Paganis^{1D}, X.f. Su^{1D}, J. Thomas-Wilsker^{1D}, L.s. Tsai, D. Tsionou, H.y. Wu, E. Yazgan^{1D}

High Energy Physics Research Unit, Department of Physics, Faculty of Science, Chulalongkorn University, Bangkok, Thailand

C. Asawatangtrakuldee^{1D}, N. Srimanobhas^{1D}, V. Wachirapusanand^{1D}

Cukurova University, Physics Department, Science and Art Faculty, Adana, Turkey

D. Agyel^{1D}, F. Boran^{1D}, F. Dolek^{1D}, I. Dumanoglu^{1D}⁶⁵, E. Eskut^{1D}, Y. Guler^{1D}⁶⁶, E. Gurpinar Guler^{1D}⁶⁶, C. Isik^{1D}, O. Kara, A. Kayis Topaksu^{1D}, U. Kiminsu^{1D}, Y. Komurcu^{1D}, G. Onengut^{1D}, K. Ozdemir^{1D}⁶⁷, A. Polatoz^{1D}, B. Tali^{1D}⁶⁸, U.G. Tok^{1D}, S. Turkcapar^{1D}, E. Uslan^{1D}, I.S. Zorbakir^{1D}

Middle East Technical University, Physics Department, Ankara, Turkey

G. Sokmen, M. Yalvac^{1D}⁶⁹

Bogazici University, Istanbul, Turkey

B. Akgun^{1D}, I.O. Atakisi^{1D}, E. Gülmmez^{1D}, M. Kaya^{1D}⁷⁰, O. Kaya^{1D}⁷¹, S. Tekten^{1D}⁷²

Istanbul Technical University, Istanbul, Turkey

A. Cakir^{1D}, K. Cankocak^{1D}^{65,73}, G.G. Dincer^{1D}⁶⁵, S. Sen^{1D}⁷⁴

Istanbul University, Istanbul, Turkey

O. Aydilek^{1D}⁷⁵, B. Hacisahinoglu^{1D}, I. Hos^{1D}⁷⁶, B. Kaynak^{1D}, S. Ozkorucuklu^{1D}, O. Potok^{1D}, H. Sert^{1D}, C. Simsek^{1D}, C. Zorbilmez^{1D}

Yildiz Technical University, Istanbul, Turkey

S. Cerci^{1D}, B. Isildak^{1D}⁷⁷, D. Sunar Cerci^{1D}, T. Yetkin^{1D}

**Institute for Scintillation Materials of National Academy of Science of Ukraine,
Kharkiv, Ukraine**

A. Boyaryntsev , B. Grynyov 

**National Science Centre, Kharkiv Institute of Physics and Technology, Kharkiv,
Ukraine**

L. Levchuk 

University of Bristol, Bristol, United Kingdom

D. Anthony , J.J. Brooke , A. Bundock , F. Bury , E. Clement , D. Cussans , H. Flacher , M. Glowacki , J. Goldstein , H.F. Heath , M.-L. Holmberg , L. Kreczko , S. Paramesvaran , L. Robertshaw , S. Seif El Nasr-Storey , V.J. Smith , N. Stylianou ⁷⁸, K. Walkingshaw Pass

Rutherford Appleton Laboratory, Didcot, United Kingdom

A.H. Ball , K.W. Bell , A. Belyaev ⁷⁹, C. Brew , R.M. Brown , D.J.A. Cockerill , C. Cooke , A. Elliot , K.V. Ellis , K. Harder , S. Harper , J. Linacre , K. Manolopoulos , D.M. Newbold , E. Olaiya , D. Petyt , T. Reis , A.R. Sahasransu , G. Salvi , T. Schuh , C.H. Shepherd-Themistocleous , I.R. Tomalin , K.C. Whalen , T. Williams

Imperial College, London, United Kingdom

I. Andreou , R. Bainbridge , P. Bloch , C.E. Brown , O. Buchmuller , V. Cacchio , C.A. Carrillo Montoya , G.S. Chahal ⁸⁰, D. Colling , J.S. Dancu , I. Das , P. Dauncey , G. Davies , J. Davies , M. Della Negra , S. Fayer , G. Fedi , G. Hall , M.H. Hassanshahi , A. Howard , G. Iles , C.R. Knight , J. Langford , J. León Holgado , L. Lyons , A.-M. Magnan , B. Maier , S. Mallios , M. Mieskolainen , J. Nash ⁸¹, M. Pesaresi , P.B. Pradeep , B.C. Radburn-Smith , A. Richards , A. Rose , K. Savva , C. Seez , R. Shukla , A. Tapper , K. Uchida , G.P. Uttley , L.H. Vage , T. Virdee ³¹, M. Vojinovic , N. Wardle , D. Winterbottom

Brunel University, Uxbridge, United Kingdom

J.E. Cole , A. Khan , P. Kyberd , I.D. Reid 

Baylor University, Waco, Texas, U.S.A.

S. Abdullin , A. Brinkerhoff , E. Collins , M.R. Darwish , J. Dittmann , K. Hatakeyama , J. Hiltbrand , B. McMaster , J. Samudio , S. Sawant , C. Sutantawibul , J. Wilson 

Catholic University of America, Washington, DC, U.S.A.

R. Bartek , A. Dominguez , A.E. Simsek 

The University of Alabama, Tuscaloosa, Alabama, U.S.A.

B. Bam , A. Buchot Perraguin , R. Chudasama , S.I. Cooper , C. Crovella , S.V. Gleyzer , E. Pearson , C.U. Perez , P. Rumerio ⁸², E. Usai , R. Yi 

Boston University, Boston, Massachusetts, U.S.A.

A. Akpinar , C. Cosby , G. De Castro , Z. Demiragli , C. Erice , C. Fangmeier , C. Fernandez Madrazo , E. Fontanesi , D. Gastler , F. Golf , S. Jeon , J. O'cain , I. Reed , J. Rohlf , K. Salyer , D. Sperka , D. Spitzbart , I. Suarez , A. Tsatsos , A.G. Zecchinelli

Brown University, Providence, Rhode Island, U.S.A.

G. Benelli^{ID}, D. Cutts^{ID}, L. Gouskos^{ID}, M. Hadley^{ID}, U. Heintz^{ID}, J.M. Hogan^{ID}⁸³, T. Kwon^{ID}, G. Landsberg^{ID}, K.T. Lau^{ID}, D. Li^{ID}, J. Luo^{ID}, S. Mondal^{ID}, N. Pervan^{ID}, T. Russell, S. Sagir^{ID}⁸⁴, X. Shen, F. Simpson^{ID}, M. Stamenkovic^{ID}, N. Venkatasubramanian, X. Yan^{ID}

University of California, Davis, Davis, California, U.S.A.

S. Abbott^{ID}, C. Brainerd^{ID}, R. Breedon^{ID}, H. Cai^{ID}, M. Calderon De La Barca Sanchez^{ID}, M. Chertok^{ID}, M. Citron^{ID}, J. Conway^{ID}, P.T. Cox^{ID}, R. Erbacher^{ID}, F. Jensen^{ID}, O. Kukral^{ID}, G. Mocellin^{ID}, M. Mulhearn^{ID}, S. Ostrom^{ID}, W. Wei^{ID}, S. Yoo^{ID}, F. Zhang^{ID}

University of California, Los Angeles, California, U.S.A.

M. Bachtis^{ID}, R. Cousins^{ID}, A. Datta^{ID}, G. Flores Avila^{ID}, J. Hauser^{ID}, M. Ignatenko^{ID}, M.A. Iqbal^{ID}, T. Lam^{ID}, E. Manca^{ID}, A. Nunez Del Prado, D. Saltzberg^{ID}, V. Valuev^{ID}

University of California, Riverside, Riverside, California, U.S.A.

R. Clare^{ID}, J.W. Gary^{ID}, M. Gordon, G. Hanson^{ID}, W. Si^{ID}

University of California, San Diego, La Jolla, California, U.S.A.

A. Aportela, A. Arora^{ID}, J.G. Branson^{ID}, S. Cittolin^{ID}, S. Cooperstein^{ID}, D. Diaz^{ID}, J. Duarte^{ID}, L. Giannini^{ID}, Y. Gu, J. Guiang^{ID}, R. Kansal^{ID}, V. Krutelyov^{ID}, R. Lee^{ID}, J. Letts^{ID}, M. Masciovecchio^{ID}, F. Mokhtar^{ID}, S. Mukherjee^{ID}, M. Pieri^{ID}, M. Quinnan^{ID}, B.V. Sathia Narayanan^{ID}, V. Sharma^{ID}, M. Tadel^{ID}, E. Vourliotis^{ID}, F. Würthwein^{ID}, Y. Xiang^{ID}, A. Yagil^{ID}

University of California, Santa Barbara — Department of Physics, Santa Barbara, California, U.S.A.

A. Barzdukas^{ID}, L. Brennan^{ID}, C. Campagnari^{ID}, K. Downham^{ID}, C. Grieco^{ID}, J. Incandela^{ID}, J. Kim^{ID}, A.J. Li^{ID}, P. Masterson^{ID}, H. Mei^{ID}, J. Richman^{ID}, S.N. Santpur^{ID}, U. Sarica^{ID}, R. Schmitz^{ID}, F. Setti^{ID}, J. Sheplock^{ID}, D. Stuart^{ID}, T.Á. Vámi^{ID}, S. Wang^{ID}, D. Zhang

California Institute of Technology, Pasadena, California, U.S.A.

S. Bhattacharya^{ID}, A. Bornheim^{ID}, O. Cerri, A. Latorre, J. Mao^{ID}, H.B. Newman^{ID}, G. Reales Gutiérrez, M. Spiropulu^{ID}, J.R. Vlimant^{ID}, C. Wang^{ID}, S. Xie^{ID}, R.Y. Zhu^{ID}

Carnegie Mellon University, Pittsburgh, Pennsylvania, U.S.A.

J. Alison^{ID}, S. An^{ID}, P. Bryant^{ID}, M. Cremonesi, V. Dutta^{ID}, T. Ferguson^{ID}, T.A. Gómez Espinosa^{ID}, A. Harilal^{ID}, A. Kallil Tharayil, C. Liu^{ID}, T. Mudholkar^{ID}, S. Murthy^{ID}, P. Palit^{ID}, K. Park, M. Paulini^{ID}, A. Roberts^{ID}, A. Sanchez^{ID}, W. Terrill^{ID}

University of Colorado Boulder, Boulder, Colorado, U.S.A.

J.P. Cumalat^{ID}, W.T. Ford^{ID}, A. Hart^{ID}, A. Hassani^{ID}, G. Karathanasis^{ID}, N. Manganelli^{ID}, J. Pearkes^{ID}, C. Savard^{ID}, N. Schonbeck^{ID}, K. Stenson^{ID}, K.A. Ulmer^{ID}, S.R. Wagner^{ID}, N. Zipper^{ID}, D. Zuolo^{ID}

Cornell University, Ithaca, New York, U.S.A.

J. Alexander¹⁰, S. Bright-Thonney¹⁰, X. Chen¹⁰, D.J. Cranshaw¹⁰, J. Fan¹⁰, X. Fan¹⁰, S. Hogan¹⁰, P. Kotamnives, J. Monroy¹⁰, M. Oshiro¹⁰, J.R. Patterson¹⁰, M. Reid¹⁰, A. Ryd¹⁰, J. Thom¹⁰, P. Wittich¹⁰, R. Zou¹⁰

Fermi National Accelerator Laboratory, Batavia, Illinois, U.S.A.

M. Albrow¹⁰, M. Alyari¹⁰, O. Amram¹⁰, G. Apollinari¹⁰, A. Apresyan¹⁰, L.A.T. Bauerick¹⁰, D. Berry¹⁰, J. Berryhill¹⁰, P.C. Bhat¹⁰, K. Burkett¹⁰, J.N. Butler¹⁰, A. Canepa¹⁰, G.B. Cerati¹⁰, H.W.K. Cheung¹⁰, F. Chlebana¹⁰, G. Cummings¹⁰, J. Dickinson¹⁰, I. Dutta¹⁰, V.D. Elvira¹⁰, Y. Feng¹⁰, J. Freeman¹⁰, A. Gandrakota¹⁰, Z. Gecse¹⁰, L. Gray¹⁰, D. Green, A. Grummer¹⁰, S. Grünendahl¹⁰, D. Guerrero¹⁰, O. Gutsche¹⁰, R.M. Harris¹⁰, R. Heller¹⁰, T.C. Herwig¹⁰, J. Hirschauer¹⁰, B. Jayatilaka¹⁰, S. Jindariani¹⁰, M. Johnson¹⁰, U. Joshi¹⁰, T. Klijnsma¹⁰, B. Klima¹⁰, K.H.M. Kwok¹⁰, S. Lammel¹⁰, C. Lee¹⁰, D. Lincoln¹⁰, R. Lipton¹⁰, T. Liu¹⁰, C. Madrid¹⁰, K. Maeshima¹⁰, C. Mantilla¹⁰, D. Mason¹⁰, P. McBride¹⁰, P. Merkel¹⁰, S. Mrenna¹⁰, S. Nahn¹⁰, J. Ngadiuba¹⁰, D. Noonan¹⁰, S. Norberg, V. Papadimitriou¹⁰, N. Pastika¹⁰, K. Pedro¹⁰, C. Pena¹⁰⁸⁵, F. Ravera¹⁰, A. Reinsvold Hall¹⁰⁸⁶, L. Ristori¹⁰, M. Safdari¹⁰, E. Sexton-Kennedy¹⁰, N. Smith¹⁰, A. Soha¹⁰, L. Spiegel¹⁰, S. Stoynev¹⁰, J. Strait¹⁰, L. Taylor¹⁰, S. Tkaczyk¹⁰, N.V. Tran¹⁰, L. Uplegger¹⁰, E.W. Vaandering¹⁰, I. Zoi¹⁰

University of Florida, Gainesville, Florida, U.S.A.

C. Aruta¹⁰, P. Avery¹⁰, D. Bourilkov¹⁰, P. Chang¹⁰, V. Cherepanov¹⁰, R.D. Field, C. Huh¹⁰, E. Koenig¹⁰, M. Kolosova¹⁰, J. Konigsberg¹⁰, A. Korytov¹⁰, K. Matchev¹⁰, N. Menendez¹⁰, G. Mitselman¹⁰, K. Mohrman¹⁰, A. Muthirakalayil Madhu¹⁰, N. Rawal¹⁰, S. Rosenzweig¹⁰, Y. Takahashi¹⁰, J. Wang¹⁰

Florida State University, Tallahassee, Florida, U.S.A.

T. Adams¹⁰, A. Al Kadhim¹⁰, A. Askew¹⁰, S. Bower¹⁰, V. Hagopian¹⁰, R. Hashmi¹⁰, R.S. Kim¹⁰, S. Kim¹⁰, T. Kolberg¹⁰, G. Martinez, H. Prosper¹⁰, P.R. Prova, M. Wulansatiti¹⁰, R. Yohay¹⁰, J. Zhang

Florida Institute of Technology, Melbourne, Florida, U.S.A.

B. Alsufyani, M.M. Baarmand¹⁰, S. Butalla¹⁰, S. Das¹⁰, T. Elkafrawy¹⁰¹⁸, M. Hohlmann¹⁰, E. Yanes

University of Illinois Chicago, Chicago, Illinois, U.S.A.

M.R. Adams¹⁰, A. Baty¹⁰, C. Bennett, R. Cavanaugh¹⁰, R. Escobar Franco¹⁰, O. Evdokimov¹⁰, C.E. Gerber¹⁰, M. Hawksworth, A. Hingrajiya, D.J. Hofman¹⁰, J.h. Lee¹⁰, D. S. Lemos¹⁰, A.H. Merrit¹⁰, C. Mills¹⁰, S. Nanda¹⁰, G. Oh¹⁰, B. Ozek¹⁰, D. Pilipovic¹⁰, R. Pradhan¹⁰, E. Prifti, T. Roy¹⁰, S. Rudrabhatla¹⁰, N. Singh, M.B. Tonjes¹⁰, N. Varelas¹⁰, M.A. Wadud¹⁰, Z. Ye¹⁰, J. Yoo¹⁰

The University of Iowa, Iowa City, Iowa, U.S.A.

M. Alhusseini¹⁰, D. Blend, K. Dilsiz¹⁰⁸⁷, L. Emediato¹⁰, G. Karaman¹⁰, O.K. Köseyan¹⁰, J.-P. Merlo, A. Mestvirishvili¹⁰⁸⁸, O. Neogi, H. Ogul¹⁰⁸⁹, Y. Onel¹⁰, A. Penzo¹⁰, C. Snyder, E. Tiras¹⁰⁹⁰

Johns Hopkins University, Baltimore, Maryland, U.S.A.

B. Blumenfeld , L. Corcodilos , J. Davis , A.V. Gritsan , L. Kang , S. Kyriacou , P. Maksimovic , M. Roguljic , J. Roskes , S. Sekhar , M. Swartz

The University of Kansas, Lawrence, Kansas, U.S.A.

A. Abreu , L.F. Alcerro Alcerro , J. Anguiano , S. Arteaga Escatel , P. Baringer , A. Bean , Z. Flowers , D. Grove , J. King , G. Krintiras , M. Lazarovits , C. Le Mahieu , J. Marquez , M. Murray , M. Nickel , M. Pitt , S. Popescu ⁹¹, C. Rogan , C. Royon , R. Salvatico , S. Sanders , C. Smith , G. Wilson

Kansas State University, Manhattan, Kansas, U.S.A.

B. Allmond , R. Guju Gurunadha , A. Ivanov , K. Kaadze , Y. Maravin , J. Natoli , D. Roy , G. Sorrentino 

University of Maryland, College Park, Maryland, U.S.A.

A. Baden , A. Belloni , J. Bistany-riebman, Y.M. Chen , S.C. Eno , N.J. Hadley , S. Jabeen , R.G. Kellogg , T. Koeth , B. Kronheim, Y. Lai , S. Lascio , A.C. Mignerey , S. Nabili , C. Palmer , C. Papageorgakis , M.M. Paranjpe, E. Popova ⁹², A. Shevelev , L. Wang

Massachusetts Institute of Technology, Cambridge, Massachusetts, U.S.A.

J. Bendavid , I.A. Cali , P.c. Chou , M. D'Alfonso , J. Eysermans , C. Freer , G. Gomez-Ceballos , M. Goncharov, G. Grossos, P. Harris, D. Hoang, D. Kovalskyi , J. Krupa , L. Lavezzo , Y.-J. Lee , K. Long , C. McGinn, A. Novak , M.I. Park , C. Paus , C. Reissel , C. Roland , G. Roland , S. Rothman , G.S.F. Stephans , Z. Wang , B. Wyslouch , T. J. Yang

University of Minnesota, Minneapolis, Minnesota, U.S.A.

B. Crossman , B.M. Joshi , C. Kapsiak , M. Krohn , D. Mahon , J. Mans , B. Marzocchi , M. Revering , R. Rusack , R. Saradhy , N. Strobbe

University of Nebraska-Lincoln, Lincoln, Nebraska, U.S.A.

K. Bloom , D.R. Claes , G. Haza , J. Hossain , C. Joo , I. Kravchenko , J.E. Siado , W. Tabb , A. Vagnerini , A. Wightman , F. Yan , D. Yu

State University of New York at Buffalo, Buffalo, New York, U.S.A.

H. Bandyopadhyay , L. Hay , H.w. Hsia, I. Iashvili , A. Kalogeropoulos , A. Kharchilava , M. Morris , D. Nguyen , J. Pekkanen , S. Rappoccio , H. Rejeb Sfar, A. Williams , P. Young

Northeastern University, Boston, Massachusetts, U.S.A.

G. Alverson , E. Barberis , J. Bonilla , B. Bylsma, M. Campana , J. Dervan, Y. Haddad , Y. Han , I. Israr , A. Krishna , J. Li , M. Lu , G. Madigan , R. McCarthy , D.M. Morse , V. Nguyen , T. Orimoto , A. Parker , L. Skinnari , D. Wood

Northwestern University, Evanston, Illinois, U.S.A.

J. Bueghly, S. Dittmer , K.A. Hahn , Y. Liu , M. McGinnis , Y. Miao , D.G. Monk , M.H. Schmitt , A. Taliercio , M. Velasco

University of Notre Dame, Notre Dame, Indiana, U.S.A.

G. Agarwal , R. Band , R. Bucci, S. Castells , A. Das , R. Goldouzian , M. Hildreth , K.W. Ho , K. Hurtado Anampa , T. Ivanov , C. Jessop , K. Lannon , J. Lawrence , N. Loukas , L. Lutton , J. Mariano, N. Marinelli, I. Mcalister, T. McCauley , C. McGrady , C. Moore , Y. Musienko ¹⁶, H. Nelson , M. Osherson , A. Piccinelli , R. Ruchti , A. Townsend , Y. Wan, M. Wayne , H. Yockey, M. Zarucki , L. Zygala

The Ohio State University, Columbus, Ohio, U.S.A.

A. Basnet , M. Carrigan , L.S. Durkin , C. Hill , M. Joyce , M. Nunez Ornelas , K. Wei, B.L. Winer , B. R. Yates 

Princeton University, Princeton, New Jersey, U.S.A.

H. Bouchamaoui , K. Coldham, P. Das , G. Dezoort , P. Elmer , A. Frankenthal , B. Greenberg , N. Haubrich , K. Kennedy, G. Kopp , S. Kwan , D. Lange , A. Loeliger , D. Marlow , I. Ojalvo , J. Olsen , D. Stickland , C. Tully

University of Puerto Rico, Mayaguez, Puerto Rico, U.S.A.

S. Malik 

Purdue University, West Lafayette, Indiana, U.S.A.

A.S. Bakshi , S. Chandra , R. Chawla , A. Gu , L. Gutay, M. Jones , A.W. Jung , A.M. Koshy, M. Liu , G. Negro , N. Neumeister , G. Paspalaki , S. Piperov , V. Scheurer, J.F. Schulte , M. Stojanovic , J. Thieman , A. K. Virdi , F. Wang , A. Wildridge , W. Xie , Y. Yao

Purdue University Northwest, Hammond, Indiana, U.S.A.

J. Dolen , N. Parashar , A. Pathak 

Rice University, Houston, Texas, U.S.A.

D. Acosta , T. Carnahan , K.M. Ecklund , P.J. Fernández Manteca , S. Freed, P. Gardner, F.J.M. Geurts , I. Krommydas , W. Li , J. Lin , O. Miguel Colin , B.P. Padley , R. Redjimi, J. Rotter , E. Yigitbasi , Y. Zhang

University of Rochester, Rochester, New York, U.S.A.

A. Bodek , P. de Barbaro , R. Demina , J.L. Dulemba , A. Garcia-Bellido , O. Hindrichs , A. Khukhunaishvili , N. Parmar, P. Parygin ⁹², R. Taus 

Rutgers, The State University of New Jersey, Piscataway, New Jersey, U.S.A.

B. Chiarito, J.P. Chou , S.V. Clark , D. Gadkari , Y. Gershtein , E. Halkiadakis , M. Heindl , C. Houghton , D. Jaroslawski , S. Konstantinou , I. Laflotte , A. Lath , R. Montalvo, K. Nash, J. Reichert , H. Routray , P. Saha , S. Salur , S. Schnetzer, S. Somalwar , R. Stone , S.A. Thayil , S. Thomas, J. Vora , H. Wang

University of Tennessee, Knoxville, Tennessee, U.S.A.

D. Ally , A.G. Delannoy , S. Fiorendi , S. Higginbotham , T. Holmes , A.R. Kanuganti , N. Karunaratnha , L. Lee , E. Nibigira , S. Spanier 

Texas A&M University, College Station, Texas, U.S.A.

D. Aebi , M. Ahmad , T. Akhter , K. Androsov ⁶⁰, O. Bouhalil  ⁹³, R. Eusebi , J. Gilmore , T. Huang , T. Kamon  ⁹⁴, H. Kim , S. Luo , R. Mueller , D. Overton , D. Rathjens , A. Safonov

Texas Tech University, Lubbock, Texas, U.S.A.

N. Akchurin , J. Damgov , N. Gogate , V. Hegde , A. Hussain , Y. Kazhykarim, K. Lamichhane , S.W. Lee , A. Mankel , T. Peltola , I. Volobouev 

Vanderbilt University, Nashville, Tennessee, U.S.A.

E. Appelt , Y. Chen , S. Greene, A. Gurrola , W. Johns , R. Kunawalkam Elayavalli , A. Melo , F. Romeo , P. Sheldon , S. Tuo , J. Velkovska , J. Viinikainen 

University of Virginia, Charlottesville, Virginia, U.S.A.

B. Cardwell , H. Chung, B. Cox , J. Hakala , R. Hirosky , A. Ledovskoy , C. Neu 

Wayne State University, Detroit, Michigan, U.S.A.

S. Bhattacharya , P.E. Karchin 

University of Wisconsin — Madison, Madison, Wisconsin, U.S.A.

A. Aravind, S. Banerjee , K. Black , T. Bose , E. Chavez, S. Dasu , I. De Bruyn , P. Everaerts , C. Galloni, H. He , M. Herndon , A. Herve , C.K. Koraka , A. Lanaro, R. Loveless , J. Madhusudanan Sreekala , A. Mallampalli , A. Mohammadi , S. Mondal, G. Parida , L. Pétré , D. Pinna, A. Savin, V. Shang , V. Sharma , W.H. Smith , D. Teague, H.F. Tsui , W. Vetens , A. Warden 

Authors affiliated with an institute or an international laboratory covered by a cooperation agreement with CERN

S. Afanasiev , V. Alexakhin , D. Budkouski , I. Golutvin  [†], I. Gorbunov , V. Karjavine , V. Korenkov , A. Lanev , A. Malakhov , V. Matveev  ⁹⁵, V. Palichik , V. Perelygin , M. Savina , V. Shalaev , S. Shmatov , S. Shulha , V. Smirnov , O. Teryaev , N. Voytishin , B.S. Yuldashev  ⁹⁶, A. Zarubin , I. Zhizhin , G. Gavrilov , V. Golovtcov , Y. Ivanov , V. Kim  ⁹⁵, P. Levchenko  ⁹⁷, V. Murzin , V. Oreshkin , D. Sosnov , V. Sulimov , L. Uvarov , A. Vorobyev [†], Yu. Andreev , A. Dermenev , S. Gnnienko , N. Golubev , A. Karneyeu , D. Kirpichnikov , M. Kirsanov , N. Krasnikov , I. Tlisova , A. Toropin , T. Aushev , V. Gavrilov , N. Lychkovskaya , A. Nikitenko  ^{98,99}, V. Popov , A. Zhokin , R. Chistov  ⁹⁵, M. Danilov  ⁹⁵, S. Polikarpov  ⁹⁵, V. Andreev , M. Azarkin , M. Kirakosyan, A. Terkulov , E. Boos , V. Bunichev , M. Dubinin  ⁸⁵, L. Dudko , A. Gribushin , V. Klyukhin , A. Markina, S. Obraztsov , M. Perfilov, V. Savrin , P. Volkov , G. Vorotnikov , V. Blinov  ⁹⁵, T. Dimova  ⁹⁵, A. Kozyrev  ⁹⁵, O. Radchenko  ⁹⁵, Y. Skovpen  ⁹⁵, V. Kachanov , D. Konstantinov , S. Slabospitskii , A. Uzunian , A. Babaev , V. Borshch , D. Druzhkin  ¹⁰⁰

Authors affiliated with an institute formerly covered by a cooperation agreement with CERN

V. Chekhovsky, V. Makarenko 

[†] Deceased

- ¹ Also at Yerevan State University, Yerevan, Armenia
- ² Also at TU Wien, Vienna, Austria
- ³ Also at Ghent University, Ghent, Belgium
- ⁴ Also at Universidade do Estado do Rio de Janeiro, Rio de Janeiro, Brazil
- ⁵ Also at Universidade Estadual de Campinas, Campinas, Brazil
- ⁶ Also at Federal University of Rio Grande do Sul, Porto Alegre, Brazil
- ⁷ Also at UFMS, Nova Andradina, Brazil
- ⁸ Also at University of Chinese Academy of Sciences, Beijing, China
- ⁹ Also at China Center of Advanced Science and Technology, Beijing, China
- ¹⁰ Also at University of Chinese Academy of Sciences, Beijing, China
- ¹¹ Also at China Spallation Neutron Source, Guangdong, China
- ¹² Now at Henan Normal University, Xinxiang, China
- ¹³ Also at Nanjing Normal University, Nanjing, China
- ¹⁴ Now at The University of Iowa, Iowa City, Iowa, U.S.A.
- ¹⁵ Also at Université Libre de Bruxelles, Bruxelles, Belgium
- ¹⁶ Also at an institute or an international laboratory covered by a cooperation agreement with CERN
- ¹⁷ Also at Cairo University, Cairo, Egypt
- ¹⁸ Also at Ain Shams University, Cairo, Egypt
- ¹⁹ Also at Suez University, Suez, Egypt
- ²⁰ Now at British University in Egypt, Cairo, Egypt
- ²¹ Also at Purdue University, West Lafayette, Indiana, U.S.A.
- ²² Also at Université de Haute Alsace, Mulhouse, France
- ²³ Also at İstinye University, Istanbul, Turkey
- ²⁴ Also at Tbilisi State University, Tbilisi, Georgia
- ²⁵ Also at The University of the State of Amazonas, Manaus, Brazil
- ²⁶ Also at University of Hamburg, Hamburg, Germany
- ²⁷ Also at RWTH Aachen University, III. Physikalisches Institut A, Aachen, Germany
- ²⁸ Also at Bergische University Wuppertal (BUW), Wuppertal, Germany
- ²⁹ Also at Brandenburg University of Technology, Cottbus, Germany
- ³⁰ Also at Forschungszentrum Jülich, Juelich, Germany
- ³¹ Also at CERN, European Organization for Nuclear Research, Geneva, Switzerland
- ³² Also at Institute of Nuclear Research ATOMKI, Debrecen, Hungary
- ³³ Now at Universitatea Babes-Bolyai — Facultatea de Fizica, Cluj-Napoca, Romania
- ³⁴ Also at MTA-ELTE Lendület CMS Particle and Nuclear Physics Group, Eötvös Loránd University, Budapest, Hungary
- ³⁵ Also at HUN-REN Wigner Research Centre for Physics, Budapest, Hungary
- ³⁶ Also at Physics Department, Faculty of Science, Assiut University, Assiut, Egypt
- ³⁷ Also at Punjab Agricultural University, Ludhiana, India
- ³⁸ Also at University of Visva-Bharati, Santiniketan, India
- ³⁹ Also at Indian Institute of Science (IISc), Bangalore, India
- ⁴⁰ Also at IIT Bhubaneswar, Bhubaneswar, India
- ⁴¹ Also at Institute of Physics, Bhubaneswar, India
- ⁴² Also at University of Hyderabad, Hyderabad, India
- ⁴³ Also at Deutsches Elektronen-Synchrotron, Hamburg, Germany
- ⁴⁴ Also at Isfahan University of Technology, Isfahan, Iran
- ⁴⁵ Also at Sharif University of Technology, Tehran, Iran
- ⁴⁶ Also at Department of Physics, University of Science and Technology of Mazandaran, Behshahr, Iran
- ⁴⁷ Also at Department of Physics, Faculty of Science, Arak University, ARAK, Iran
- ⁴⁸ Also at Helwan University, Cairo, Egypt
- ⁴⁹ Also at Italian National Agency for New Technologies, Energy and Sustainable Economic Development, Bologna, Italy
- ⁵⁰ Also at Centro Siciliano di Fisica Nucleare e di Struttura Della Materia, Catania, Italy

- ⁵¹ Also at Università degli Studi Guglielmo Marconi, Roma, Italy
⁵² Also at Scuola Superiore Meridionale, Università di Napoli ‘Federico II’, Napoli, Italy
⁵³ Also at Fermi National Accelerator Laboratory, Batavia, Illinois, U.S.A.
⁵⁴ Also at Consiglio Nazionale delle Ricerche — Istituto Officina dei Materiali, Perugia, Italy
⁵⁵ Also at Department of Applied Physics, Faculty of Science and Technology, Universiti Kebangsaan Malaysia, Bangi, Malaysia
⁵⁶ Also at Consejo Nacional de Ciencia y Tecnología, Mexico City, Mexico
⁵⁷ Also at Trincomalee Campus, Eastern University, Sri Lanka, Nilaveli, Sri Lanka
⁵⁸ Also at Saegis Campus, Nugegoda, Sri Lanka
⁵⁹ Also at National and Kapodistrian University of Athens, Athens, Greece
⁶⁰ Also at Ecole Polytechnique Fédérale Lausanne, Lausanne, Switzerland
⁶¹ Also at University of Vienna, Vienna, Austria
⁶² Also at Universität Zürich, Zurich, Switzerland
⁶³ Also at Stefan Meyer Institute for Subatomic Physics, Vienna, Austria
⁶⁴ Also at Laboratoire d’Annecy-le-Vieux de Physique des Particules, IN2P3-CNRS, Annecy-le-Vieux, France
⁶⁵ Also at Near East University, Research Center of Experimental Health Science, Mersin, Turkey
⁶⁶ Also at Konya Technical University, Konya, Turkey
⁶⁷ Also at Izmir Bakircay University, Izmir, Turkey
⁶⁸ Also at Adiyaman University, Adiyaman, Turkey
⁶⁹ Also at Bozok Universitetesi Rektörlüğü, Yozgat, Turkey
⁷⁰ Also at Marmara University, Istanbul, Turkey
⁷¹ Also at Milli Savunma University, Istanbul, Turkey
⁷² Also at Kafkas University, Kars, Turkey
⁷³ Now at Istanbul Okan University, Istanbul, Turkey
⁷⁴ Also at Hacettepe University, Ankara, Turkey
⁷⁵ Also at Erzincan Binali Yıldırım University, Erzincan, Turkey
⁷⁶ Also at Istanbul University — Cerrahpasa, Faculty of Engineering, Istanbul, Turkey
⁷⁷ Also at Yildiz Technical University, Istanbul, Turkey
⁷⁸ Also at Vrije Universiteit Brussel, Brussel, Belgium
⁷⁹ Also at School of Physics and Astronomy, University of Southampton, Southampton, United Kingdom
⁸⁰ Also at IPPP Durham University, Durham, United Kingdom
⁸¹ Also at Monash University, Faculty of Science, Clayton, Australia
⁸² Also at Università di Torino, Torino, Italy
⁸³ Also at Bethel University, St. Paul, Minnesota, U.S.A.
⁸⁴ Also at Karamanoğlu Mehmetbey University, Karaman, Turkey
⁸⁵ Also at California Institute of Technology, Pasadena, California, U.S.A.
⁸⁶ Also at United States Naval Academy, Annapolis, Maryland, U.S.A.
⁸⁷ Also at Bingöl University, Bingöl, Turkey
⁸⁸ Also at Georgian Technical University, Tbilisi, Georgia
⁸⁹ Also at Sinop University, Sinop, Turkey
⁹⁰ Also at Erciyes University, Kayseri, Turkey
⁹¹ Also at Horia Hulubei National Institute of Physics and Nuclear Engineering (IFIN-HH), Bucharest, Romania
⁹² Now at another institute or international laboratory covered by a cooperation agreement with CERN
⁹³ Also at Texas A&M University at Qatar, Doha, Qatar
⁹⁴ Also at Kyungpook National University, Daegu, Korea
⁹⁵ Also at another institute or international laboratory covered by a cooperation agreement with CERN
⁹⁶ Also at Institute of Nuclear Physics of the Uzbekistan Academy of Sciences, Tashkent, Uzbekistan
⁹⁷ Also at Northeastern University, Boston, Massachusetts, U.S.A.
⁹⁸ Also at Imperial College, London, United Kingdom
⁹⁹ Now at Yerevan Physics Institute, Yerevan, Armenia
¹⁰⁰ Also at Universiteit Antwerpen, Antwerpen, Belgium